# SYMMETRYLENS: A NEW CANDIDATE PARADIGM FOR UNSUPERVISED SYMMETRY LEARNING VIA LOCALITY AND EQUIVARIANCE

#### **Onur Efe**

Department of Physics Bogazici University Istanbul, Turkey onur.efe@bogazici.edu.tr

#### Arkadas Ozakin

Department of Physics
Bogazici University
Istanbul, Turkey
arkadas.ozakin@bogazici.edu.tr

October 8, 2024

#### **ABSTRACT**

We develop a new, unsupervised symmetry learning method that starts with raw data, and gives the minimal (discrete) generator of an underlying Lie group of symmetries, together with a symmetry equivariant representation of the data. The method is able to learn the pixel translation operator from a dataset with only an approximate translation symmetry, and can learn quite different types of symmetries which are not apparent to the naked eye, equally well. The method is based on the formulation of an information-theoretic loss function that measures both the degree to which the dataset is symmetric under a given candidate symmetry, and also, the degree of locality of the samples in the dataset with respect to this symmetry. We demonstrate that this coupling between symmetry and locality, together with a special optimization technique developed for entropy estimation, results in a highly stable system that gives reproducible results. The symmetry actions we consider are group representations, however, we believe the approach has the potential to be generalized to more general, nonlinear actions of non-commutative Lie groups.

# 1 Introduction

The spectacular success of convolutional neural networks (CNN) has triggered a wide range of approaches to their generalization. CNNs are equivariant under pixel translations, which is also a property of the information content in natural image data. By using a weight sharing scheme that respects such an underlying symmetry, it has been possible to introduce a powerful inductive bias in line with the nature of the data, resulting in highly accurate predictive models. How can this approach be generalized?

Translations form a *group*, and for the cases where a more general underlying symmetry group is known, a mathematically elegant generalization was developed in the form of *group convolutional networks*. [1] However, data often has underlying symmetries that are *not known explicitly beforehand*. In such cases, a method for *discovering* the underlying symmetry from data would be highly desirable.

Learning symmetries from data would allow one to develop an efficient weight sharing scheme as in CNNs, but even without this practical application, simply being able to discover unknown symmetries is of considerable interest in itself. In many fields, symmetries in data give deep insights into the nature of the system that produces the data. For example, in physics, continuous symmetries are closely related to conservation laws, and the knowledge of the symmetries of a mechanical system allows one to develop both analytical[2] and numerical[3] methods for investigating dynamics. More generally, the discovery of a new symmetry in a dataset would almost surely trigger research into the underlying mechanisms generating that symmetry.

In this paper, we develop a new method for discovering symmetries from raw data: For a dataset that has an underlying, unknown Lie group of symmetries (analogous to translation symmetry), the model gives a generator of the symmetry

(analogous to pixel translations). In other words, we develop an unsupervised method, which has no other tasks such as classification or regression: the data is given to the system without any labels of any sort, and out comes the symmetry operator.

In the context of symmetry learning, one sometimes restricts attention to symmetry transformations acting on samples only through actions on some underlying "coordinate" space, e.g. in the case of images, a translated image is obtained by acting the translation operator on the pixels. We would like to emphasize that our setting is more general in that we consider a symmetry group of transformations acting directly on samples, and so-called "regular representations" (of which pixel translations is an example) are only a special case of our approach.

To give some spoilers, our method is able to start with a dataset that is approximately invariant under translations as in image data, and discover the pixel translation symmetry operator. We describe our datasets in detail below, but it is worth mentioning that *approximately invariant* here means, in particular, that we do not include translated versions of individual samples (which is what one often does in data augmentation). The data comes from an underlying invariant distribution, but the training set itself is not forced to be strictly invariant.

Although this is not a straightforward task, rediscovering the familiar case of pixel translations from such a dataset is perhaps the first thing to demand of a method that claims to learn generalized symmetries from raw data. However, our approach allows the system to discover symmetries that are much less obvious.

Suppose we take a dataset that is again approximately invariant under pixel translations, and apply a fixed permutation to the pixels to obtain a new dataset. The underlying symmetry of this new dataset will be much less obvious to the naked eye—the generator of the symmetry will now be an operator like Pixel  $1 \rightarrow$  Pixel  $17 \rightarrow$  Pixel 12, etc. We demonstrate that our method can discover this symmetry just as well as it discovers pixel translation. In our experimental sections, we will give further examples of non-obvious symmetries with quite different flavors and motivations, including a symmetry that shifts the frequency components, and a symmetry related to wave propagation in a dispersive, homogeneous medium.

In the following sections we give the theoretical underpinnings of our approach and the technical details of the method itself, but the fundamental intuition is rather simple, and we next give a quick description.

Our approach is based on formulating two important properties to demand of a symmetry group for a dataset, namely, *stationarity* and *locality*, and an appropriate loss function that measures the degree to which these properties are satisfied

**Stationarity.** The first natural characteristic of a symmetry is the preservation of the underlying distribution. In other words, the original data and the transformed version should have approximately the same distribution. In the case of images, this means that the joint distribution of all pixels should be invariant under translation of pixels. In the general, continuous case, this means that the underlying stochastic process that generates the data should be "stationary" under the action of the symmetry group, which we will assume to be a Lie group. Although such a stationarity may not be obvious to the naked eye, once one knows the candidate symmetry group, one should be able to confirm the behavior.

As emphasized in, e.g., [4], the space of all density-preserving maps for a multi-dimensional dataset is large and includes maps that one would not normally want to call symmetries, so simply seeking density- (or distribution-) preserving maps will not necessarily allow one to discover symmetries. This property, nevertheless, is a characteristic that a symmetry transformation should satisfy. Implementing a loss function that gives a measure of the departure from the expected behavior will help us discover distribution-preserving transformations.

**Locality.** To identify the other fundamental property we will demand of a symmetry group, we turn back to CNNs for inspiration. A CNN model not only respects the underlying translation symmetry, but does so in a *local* way, in the sense that each filter has limited spatial extent. This inductive bias, as well, corresponds to an underlying property of image data. Images represent objects, which consist of building blocks that are spatially localized, and local filters do a good job of extracting such local information. <sup>2</sup>

While locality and symmetry are distinct properties, they are often coupled, and this coupling often hints at something fundamental about the processes generating the data. In physics, space and time translation symmetries and spacetime locality are intimately coupled, and this locality-symmetry is a fundamental property of quantum field theories describing the standard model.[5]<sup>3</sup>

<sup>&</sup>lt;sup>1</sup>Ingoring boundary effects, which we will return to below.

<sup>&</sup>lt;sup>2</sup>Localized combinations of building blocks form building blocks at a higher level, and stacked layers of CNNs make use of this underlying structure.

<sup>&</sup>lt;sup>3</sup>While translation symmetries are broken in curved spacetimes, their infinitesimal versions continue to play a significant role.

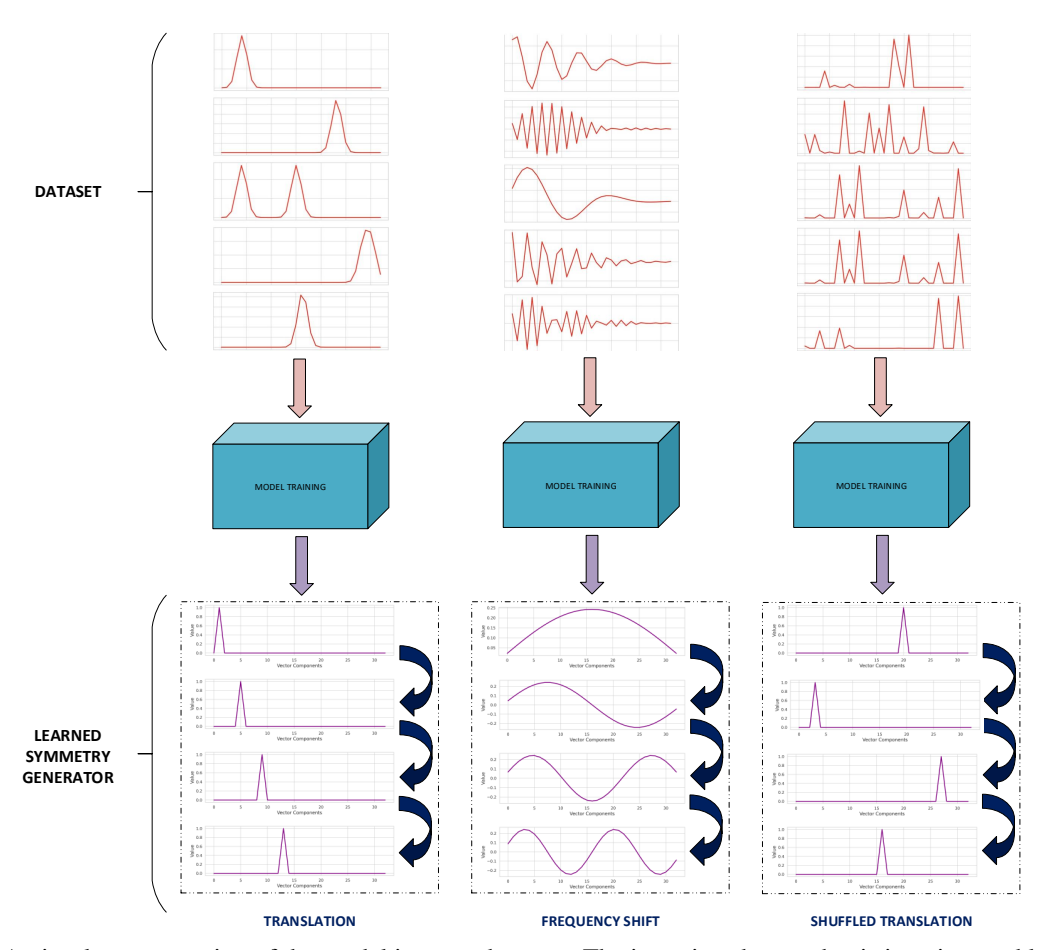


Figure 1: A visual representation of the model input and output. The input is a dataset that is invariant and local under a given group action, and the output, after training, is the learned group action. For the case on the left, the dataset is local and invariant under "1-dimensional pixel translations", i.e., the operation of sending each component of the input vector to the next, or, equivalently, sending each standard basis vector to the next one, where the ordering is the original ordering in the dataset. For the example in the middle, the dataset is local/symmetric under frequency shifts, or, equivalently, sending each Fourier basis vector to the next. In the final case, the symmetry generator sends each component to another component, but the ordering of the shifts is not as in the original ordering of the data input. The model is able to recover the given symmetry operations in each one of these example cases. For the connection of these discrete generators to the underlying Lie group, see the Methods section.

We choose to enforce a generalized notion of *locality* as the second fundamental property that the symmetry group should satisfy—the symmetry directions should be coupled to the locality directions in data. But what should this mean?

When a single, local CNN filter is applied to an image, we get a single, local scalar—a random variable that represents a small patch of the image. If we apply the same filter after translating the image slightly, we get a different random variable. If the information in images is indeed spatially local, these two random variables should be similar to each other in a strong sense. In particular, they should be strongly *dependent* random variables with similar distributions. Furthermore, as we perform further translations before applying the filter, the similarity with the original random variable should decrease.

With this motivation, we require that a general, unknown group of symmetries should satisfy a similar locality property. Suppose we are given a scalar map that is local along the unknown symmetry direction (as a CNN filter is local in the direction of pixel translations), giving us a single number for each sample. If we first apply a small symmetry transformation<sup>4</sup> to the sample and then get this scalar representation, we should end up with a scalar that is strongly

<sup>&</sup>lt;sup>4</sup>A Lie group element will be called small if it is near the identity element.

similar to the original scalar as a random variable. However, as we repeat the procedure with larger symmetries, the similarity should go down.

A loss function that utilizes such a fixed, local scalar representation to give a measure the similarity between the scalar and its transformed versions (under the candidate group elements) should thus help us find symmetry groups that have the required coupling with locality.

However, there is a chicken-egg problem here: to do our search for symmetry, we need a scalar representation which itself is local along the symmetry direction. But before the symmetry group is known, this direction of filter locality is also unknown. In other words, we do not know how to find a local filter to use in our search for symmetry before knowing the symmetry group itself.

We solve this problem by a sort of bootstrapping: we seek the local scalar representation and the symmetry group simultaneously and self-consistently in our optimization by using an appropriate loss function that applies to both.<sup>5</sup> As described below, this coupled search for a local filter and the symmetry group also gives us a group-equivariant representation of the data; in a way, the analogue of a CNN layer.

We emphasize from the outset that we do not assume the data space to be a so-called homogeneous space under the action of the Lie group of symmetries. More explicitly, we do not assume that the symmetry group is large enough to map any given point in the sample space to any other point. This would be a highly restrictive assumption, which is not, for example, satisfied by image data.

See Figure 2 for an intuitive example of the type of data/symmetry setting we assume.

We find it highly satisfying that the approach described above actually works. But the devil, unsurprisingly, is in the details. The dynamics of the optimization of a loss function is complicated, and various seemingly similar implementations of the same intuition can result in widely varying results. The method we detail in the following sections is a specific implementation of the ideas of locality and stationarity described above, and it results in a highly accurate and *stable* system that that gives reproducible results.

As a summary, the main contributions of the paper are

- A new, unsupervised symmetry learning approach that learns the generator of an underlying Lie group action
  that is able to recover pixel translations from a dataset that is only approximately invariant under pixel
  translations.
- Demonstration of the symmetry recovery capabilities on quite different sorts of examples.
- The formulation of a new approach to symmetry learning consisting of learning maps that respect both symmetry and locality, coupled in a natural way.
- The formulation of an information-theoretic loss function encapsulating the symmetry and locality properties.
- The development of optimization techniques ("time-dependent rank", see Section 3.6.2) that help the model avoid local minima, and result in robust, reproducible results.
- A resulting data representation that can be used as input to a regular CNN, thus allowing the model to work as an adaptor between raw data and the whole machinery of CNNs.

#### 2 Related work

Symmetry learning in neural networks is a rapidly evolving area of research, driven both by the value of symmetries for natural sciences and by the introduction of inductive biases to model architectures. The current literature involves nuanced definitions for the symmetry learning problem as well as different symmetry learning schemes. This section reviews current studies organized with respect to the symmetry learning scheme they proposed.

Supervised learning based approaches have been explored for learning symmetries in different contexts. One line of study is oriented towards learning symmetry transformations over image coordinates  $(2 \times 2 \text{ matrices})$ . [6] propose a method for learning invariances by averaging the network's output across various symmetry transformations applied to the input. They extend this idea to learn equivariances as well while Romero et al. [7] focus on learning proper powers of symmetry generators, addressing the issue of partial equivariances where certain transformations (e.g. rotation of the digits 9 to 6) alter the meaning of the data.

<sup>&</sup>lt;sup>5</sup>We consider a single scalar filter but the method has no intrinsic limitations in this regard; it can be used with multiple filters as well.

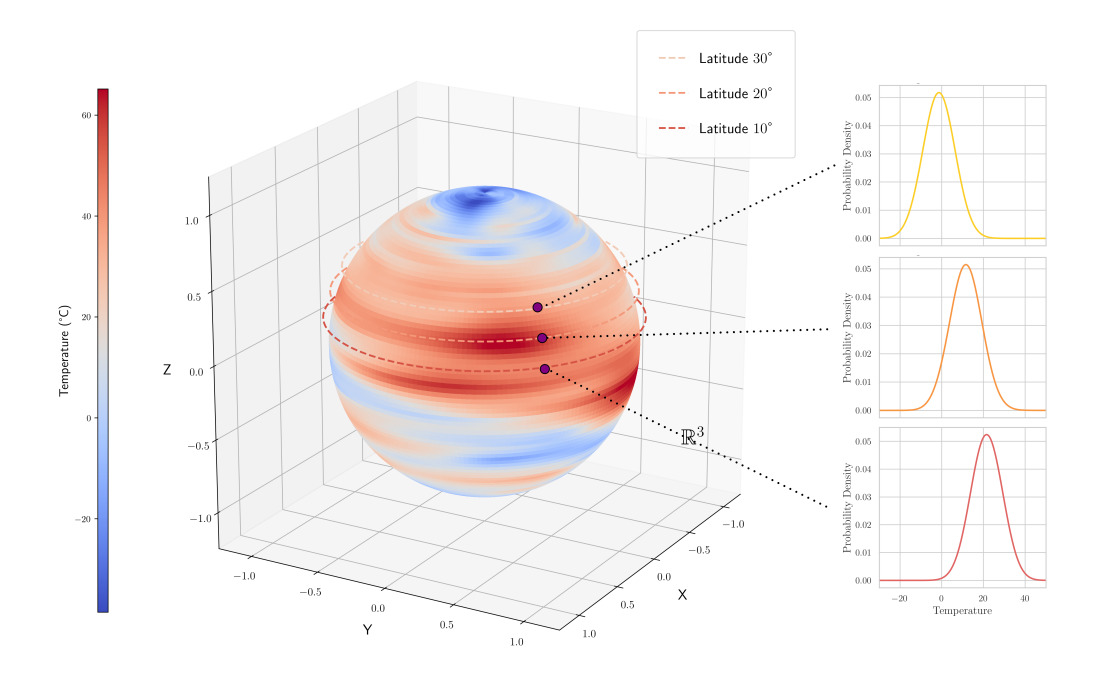


Figure 2: An example setting with a 1-parameter Lie group of symmetry and locality. The sphere represents an idealized form of the Earth, and the color coding represents the temperature distribution at a given instant. In this idealized setting, the latitude is the only variable the temperature distribution at a point depends on. More specifically, the temperature is modeled as a stochastic process on the sphere with a symmetry under azimuthal rotations. The 1-dimensional plots on the right show the probability densities of the temperature at three given locations. Moving the locations (indicated by dark dots) along their corresponding parallels would not change the density plots, since the process is symmetric under such rotations. However, locations on different parallels will have different temperature distributions (it is hotter near the equator, etc.)

Another supervised approach to symmetry learning involves the use of explicit functions that are interpolated by neural networks from the data to determine invariances[8] and [9, 10]. Given the invariant functions, the main problem becomes learning the transformations which keep their value constant.

There are also unconventional approaches based on investigating the last hidden layer of a supervised classifier and seeking ways to extract symmetry from there. [11] cluster input samples using their representations in the embedding layer to detect which samples are related by a symmetry transformation. After determining the related samples, they infer that the symmetry transformation can be easily found. [12] uses hidden layer to detect repeating patterns in an image. However, both methods require human labor.

The last approach to be mentioned involves using a set of supervised learning tasks to learn symmetry groups [13]. In this way, supervised learning tasks dictate weight-sharing mechanisms, leading to learning symmetries. The approach involves two cascaded optimization loops that lead to computationally expensive realization. In this study, it is shown that the proposed method learns translational symmetry and standard convolution under a task that requires such bias. However, the structure of the model is tuned accordingly by constraining the filter size (width of 3 pixels), which would not be the case for the general symmetry learning problem.<sup>6</sup>

Generator-Discriminator based approaches are inspired from Generative Adversarial Networks (GAN) [14] and have been used to discover symmetries of the probability distribution of data. [4] introduced SymmetryGAN, where an orthogonal symmetry generator is jointly trained with a discriminator. Although inspired from the GANs, replacing the generator with a linear map leads to problems like collapsing to identity map. Besides, due to challenges related to curse of dimensionality, the method is limited to lower dimensions. However, it represents a flexible approach to symmetry learning since it does not require a structured domain to operate.

<sup>&</sup>lt;sup>6</sup>Generally, if the data is not presented in a way that is strictly linked to the symmetry of the data, implementing a local filter becomes challenging. Limiting the size of a filter forces it to be local in the domain in which the data is presented.

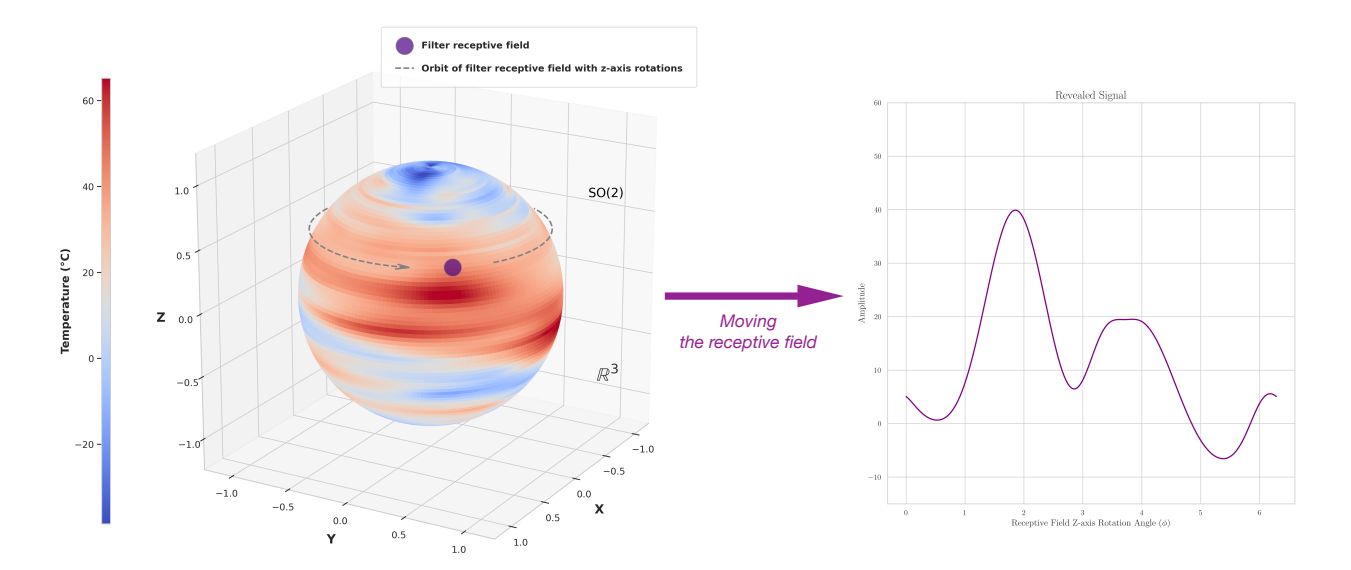


Figure 3: Observing the locality behavior by using a local, scalar filter. We use a simple averaging filter for the setting in Figure 2 to obtain a scalar from each spherical sample temperature profile, in other words, the scalar representation we use is the average temperature in the "receptive field" of the filter. If we apply a small azimuthal rotation before applying the filter, we will get the temperature at a nearby location. Since temperatures do not "jump" as one moves in the symmetry direction, the filter outputs observed by applying successive rotations will have a continuous behavior as shown on the right. This is the sense in which our model will seek a local behavior. (There is also a locality along the meridians, but there is no corresponding symmetry.)

Building on this, [15] propose enhancements such as regularization terms preventing identity collapse and sampling the group elements from distributions to discover continuous symmetries more reliably. Their follow-up work [16] extends this idea to learn approximate nonlinear groups by the use of an autoencoder. However, jointly training the discriminator, autoencoder, and generator has the potential to introduce nonexistent symmetries due to the flexibility of the autoencoder structure. Except for the autoencoder, the structure is the same as in their previous work. [15]

**Symmetry testing methods** focus on evaluating whether specific symmetries are present in a dataset instead of learning them. [17] propose an self-supervised learning approach to test for symmetries by training a discriminator to differentiate between real and transformed samples. The main idea is that, if symmetry exists, the discriminator should give a balanced output assigning equal probabilities whether or not the sample is real. The study involves calculating a score function in which higher values indicate the presence of the symmetry.

**Next-step prediction based methods** have been used for symmetry learning in the context of temporal data. [18] present an unsupervised algorithm for learning Lie group transformations from video data by maximizing the likelihood of future frames given the current one. [19] also use a similar approach in training Lie algebra convolutional networks to learn symmetries by using image pairs.

[20] and [21] introduce Hamiltonian neural networks and Noether networks, respectively, which embed physical principles such as conservation laws into neural networks motivated by learning conserved quantities instead of symmetries.

**Our method** has some similarities with the GAN-based approaches [4, 15]. Both our approach and the GAN based approaches learn symmetries based on the distribution of the data in an unsupervised manner. In addition, GANs can also learn symmetries from data with hidden structure, which is a significant advantage compared to other methods. However, since they do not have the ability to map the data to a output representation resolving independent components, they cannot learn from examples which symmetry transformations act at a local scale. Due to this problem, they cannot be used reliably for complex systems. In addition to limiting their application area to pure datasets, this also puts a severe limitation on their application over higher-dimensional spaces, since high-dimensional spaces are mostly empty due to the curse of dimensionality. This fact makes probability estimation intractable for high-dimensional datasets, which lies the foundation of GAN based methods. Since we project the data in a way that resolves local components, we can work on high-dimensional datasets solving problems related to curse of dimensionality as well as improving

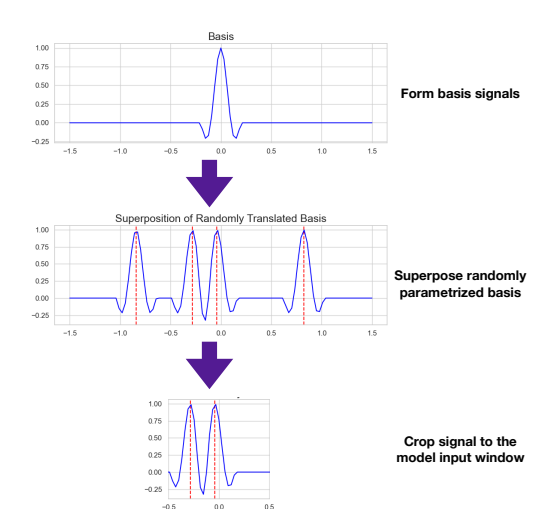


Figure 4: Data generation paradigm. We first pick a set of basis functions with parameters, then sample the parameters (such as center and width) from a given distribution with the required symmetry properties, and superpose the signals, and finally, crop the sampe to obtain an analogue of an "image". This gives a local samples whose distribution is symmetric under component ("pixel") transformations. By applying a transformation to each sample, we can create datasets that are symmetric/local under different symmetry group actions, such as frequency shifts, dispersions, etc.

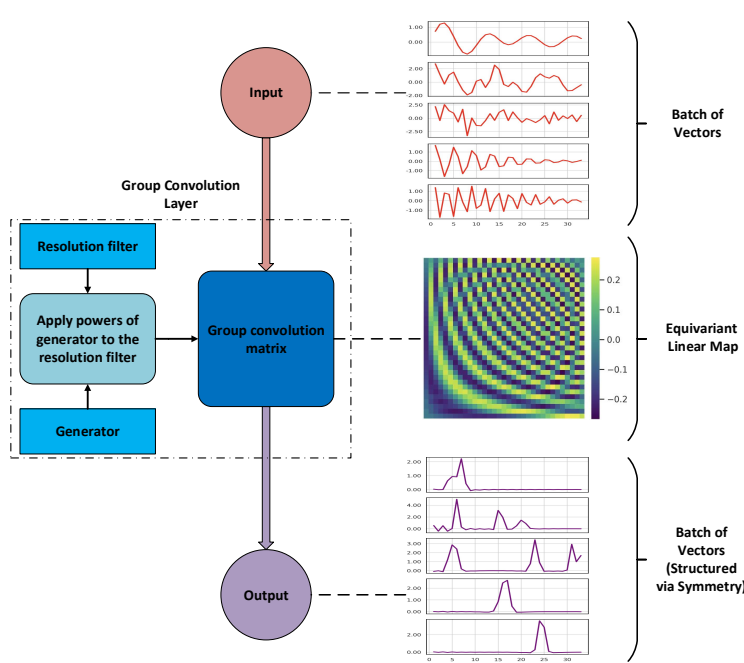


Figure 5: Overview of the method. Each sample goes through the group convolution map formed by combining the resolving filter with powers of the candidate symmetry transformation. The locality and symmetry losses are applied to the resulting representation. In the case shown here, the samples are local/symmetric under frequency shifts, and the group convolution matrix learned is effectively the matrix representing the discrete sine transform.

robustness to noise by using projections. Consequently, while the highest-dimensional learned symmetry generator for GAN based methods is a  $4 \times 4$  matrix, our method is shown to work stable with generators of  $33 \times 33$  dimensions. <sup>7</sup>

Our equivariant map has a structure similar to that of the study[13]. However, the use of Lie generators, training objectives, and the network architecture is completely different. In addition, their method is supervised, while ours works in an unsupervised manner.

Supervised methods and next-step prediction-based methods can also work in high dimensions. Although supervised learning methods are appropriate for investigating known physical systems, they are not convenient for discovering symmetries from data without such prior knowledge. On the other hand, next-step prediction works in an unsupervised manner but they require structured(temporal) data to operate. In addition, they learn one type of symmetry: time-translation symmetries, which limits their applications.

To our knowledge, we have a unique contribution related to revealing hidden manifolds in the data using a symmetry group.<sup>8</sup>

# 3 Methods

#### 3.1 Data model

In this section, we describe a theoretical setting for the types of data generating mechanisms that we will consider. We will start with a simple setting and then describe generalizations where our method applies equally well.

<sup>&</sup>lt;sup>7</sup>There are examples of independently trained generators of which form  $4 \times 4$  matrices. However, this problem has the same difficulty level as training a single generator  $4 \times 4$  in addition to the computational costs.

<sup>&</sup>lt;sup>8</sup>[16] aims to learn characteristics of equivariant representations from the data. However, in our method, we are capable of obtaining the true form of the hidden structure up to a sign and reflection.

Consider a real-valued, stationary stochastic process in one dimension. Intuitively, a stochastic process is a machine that gives us a random function  $f: \mathbb{R} \to \mathbb{R}$  (using an underlying distribution) each time we press a button. A stationary process is one where a specific sample function f(t) and all its translated versions  $f(t-\tau)$ ,  $\tau \in \mathbb{R}$  are "equally likely". Of course, it doesn't make sense to talk about the probability of a single sample function, but this is a useful informal viewpoint that we will utilize below.

Stationary stochastic processes often come up in the context of examples like the Wiener process which result in highly irregular sample functions, but another kind of example is more suitable for our setting. Consider the family of real-valued functions  $F_s(x) = \cos(x-s)$  where  $s \in [0,2\pi)$ . If we use the uniform distribution on  $[0,2\pi)$  to sample s, and then get the corresponding  $F_s(x)$ , this gives a stationary stochastic process: a function and its translated versions are all "equally likely".

To obtain sample functions that are more localized, one can start with a compactly supported test function (e.g., a localized bump)  $\phi_0(x)$  instead of  $\cos(x)$ , and consider using a random variable S to translate the center  $\phi_0(x-s)$ , see Figure 4. One can't quite get a stationary process this way since it is not possible to get a random variable uniformly distributed over the whole real line. However, this a technical difficulty that can be overcome by e.g. considering a stochastic process on a "large" circle instead of  $\mathbb{R}$ , or using a stationary point process such as the Poisson process to obtain a sample of centers with a translation-invariant distribution on  $\mathbb{R}$  rather than a single center. If we want our samples to have a noise component as well, we can consider adding a sample from a white noise process on top.

Generalizing this process to multiple "basis" functions  $\phi_i$ , possibly with random scales as well as random centers (and viewing x as a spatial variable rather than time), one can create an analogue of image data. If we imagine each basis function to represent a kind of object, e.g., a  $\phi_0$  represents an apple,  $\phi_1$  represents an orange, etc., by randomly sampling the centers of such functions and adding up the resulting sample functions for each, we get an "instance" of the "world". In each such instance sampled from the underlying process, we will have different local objects at different locations. Finally, if we crop the resulting real function to a given finite interval, we get the analogue of a (1-dimensional) image of a world which has an underlying translation symmetry and information locality.

This is the intuitive view of the types of world we will assume our model will work on, however, we will consider one significant generalization of this picture: we won't assume that the symmetry and locality are defined in terms of the shifts of the original x coordinate of the process, but will allow more general actions of a 1-parameter Lie group. Our model will aim to find the hidden Lie group action under which these properties are satisfied.  $^{10}$ 

The motivation here is that we may not have chosen the original data representation (the "x" coordinate) in line with the underlying symmetric/local process generating the data—we are, after all, working on the problem of hidden, unknown symmetry in data.

One physical example of this is encountered in wave propagation in a homogeneous, dispersive medium, i.e., a medium where different frequencies move with different phase velocities. If localized sources create disturbances that move in such a 1-dimensional dispersive medium, the waveforms recorded by a local observer will be distorted versions of the original signals—each frequency component will move with a different phase velocity, and by the time they arrive at the observer, the waveform will change its shape.

If sources of a given kind are distributed spatially uniformly, the distribution of the sample waveform functions recorded by the observer will not be symmetric under simple time translations, but there will be a symmetry under a sort of "dispersive action" of a Lie group. A recorded waveform due to a source 1km away will be related to a waveform from a similar source that is 2km away by the "dispersive action" of an element of the 1- dimensional Lie group, and due to the uniform distribution of wave sources, these waveforms will be equally likely.

We leave an attempt at the rigorous mathematical formulation of the most general setting of interest to future work with mathematically sophisticated collaborators, and simply describe a data generating procedure that results in the types of examples we have in mind. Consider the type of process described in the beginning of this section, i.e., a setting with a compactly supported basis function  $\phi_0$  and a random set of centers obtained from a Poisson process. To formulate our generalization, we will need a notion of a "delta function along  $\rho$ ", which we denote by  $\delta_{\rho}(x)$ . This will be a function that is sharply localized in the  $\rho$  direction, in other words, the original function  $\delta_{\rho}(x)$  and its transformed versions  $(\rho(\tau) \cdot \delta_{\rho})(x)$  under the action of  $\rho(\tau)$  have negligible overlap when  $\tau \neq 0$ 

We will not attempt to make this precise, but will simply give two informative examples: in the case of the action by spatial translations  $(\rho(\tau) \cdot f)(x) = f(x - \tau)$ , where each group element  $\tau$  can be thought of as a real number, the usual Dirac delta function  $\delta(x - x_0)$  is actually a "delta function along  $\rho$ "; shifting this delta function by  $\tau \neq 0$  gives a delta function which has no overlap with the original delta.

<sup>&</sup>lt;sup>9</sup>For a formal definition of stationary stochastic processes, see, e.g., [22].

<sup>&</sup>lt;sup>10</sup>We return to the multi-parameter generalization in our conclusion.

For the case of a frequency shift action<sup>11</sup>, we once again think of each  $\tau$  as a real number, but this time acting through  $(\rho(\tau) \cdot f)(x) = e^{-i\tau x} f(x)$ . In this case, one "delta function along  $\rho$ " will be simply  $f_{k_0}(x) = e^{ik_0x}$ . Acting on this function by  $\rho(\tau)$ , we get the function  $e^{i(k_0-\tau)x}$ , which is, by Fourier analysis, orthogonal to  $f_k(x)$  for  $\tau \neq 0$ .<sup>12</sup>

Given such a delta function, we define the following generalized version of the data generating process symmetric and local under a group action. Starting with a function f(x) generated by e.g. the process described in Figure 4, we define a sample  $\tilde{f}(x)$  as

$$\tilde{f}(x) = \int f(\tau)(\rho(\tau) \cdot \delta_{\rho})(x)d\tau \tag{1}$$

where once again we have thought of  $\tau$  as a real number, with a more general action this time. <sup>13</sup>

To make sense of this equation, consider the two cases described above. For a spatial translation symmetry,  $(\rho(\tau) \cdot g)(x) = g(x - \tau)$  for any sample function g. In this case,  $\delta_{\rho}(x)$  can be the usual Dirac delta,  $\delta(x)$ , and thus  $(\rho(\tau) \cdot \delta_{\rho})(x) = \delta(x - \tau)$ . This gives,

$$\tilde{f}(x) = \int f(\tau)\delta(x - \tau)d\tau = f(x)$$
(2)

Thus, we recover the original sample function, whose distribution has the locality and symmetry properties under spatial translations.

In the case of a frequency shift symmetry (for complex-valued sample functions)  $(\rho(\tau) \cdot g)(x) = e^{-i\tau x}g(x)$ , taking the delta function given above with  $k_0 = 0$ , we get  $\delta_{\rho}(x) = 1$ , and thus  $(\rho(\tau) \cdot \delta_{\rho})(x) = e^{-i\tau x}$ . This gives,

$$\tilde{f}(x) = \int f(\tau)e^{-i\tau x}d\tau \tag{3}$$

Thus, to get a stochastic process invariant and local under frequency shifts, we can simply start with a spatially local and stationary process and take the Fourier transform of each sample.

In our experiments, we will generate data with various choices for the group action using a discrete version of the process described above. In particular, we will be summing over a discrete set of group elements instead of taking an integral. We will start with a finite-dimensional sample vector  $\mathbf{v}$  which comes from a distribution with locality and symmetry under shifts of its components (e.g., a pixel shift), and use different actions  $\rho$  to generate a sample  $\tilde{\mathbf{v}}$  which is invariant and local under a different group action, provided by  $\rho$ :

$$\tilde{v}_k = \sum_p v_p(\rho(\tau_0^p) \cdot \delta_\rho)_k \tag{4}$$

where now  $\delta_{\rho}$  is a vector that represents a discrete analogue of the delta function along  $\rho$ , and  $\tau_0$  is a generator of the discrete version of the Lie group. In our experimental sections, we will focus on the case where the group action  $\rho$  is actually a group representation, i.e., for each element  $\tau$  of the 1-dimensional symmetry group, the action  $\rho(\tau)$  will be an  $n \times n$  matrix where n is the dimension of the sample vectors  $\tilde{\mathbf{v}}$ .

Learning the symmetry. Given a dataset of samples generated by a procedure similar to the one described in this section, our aim will be to reconstruct the group action  $\rho(\tau)$ . As described in the introduction to do this, we will also need to learn a "filter" that is local along the group action. The action of this filter on a sample will be a scalar, and we will enforce this scalar random variable to change little when we form it after acting on the sample by  $\rho(\tau)$  with a small  $\tau$ . If we use a large  $\tau$  to transform the sample, then the resulting scalar representation should be approximately independent of the original scalar. In a sense, then, the scalar filter to be learned will be an analogue of a "delta function along  $\rho$ " described above. We will call this filter a "resolving filter" below. Note that our setup is capable of working with multiple filters, but we will focus on the case of a single filter in this paper.

<sup>&</sup>lt;sup>11</sup>for complex-valued functions

<sup>&</sup>lt;sup>12</sup>For stochastic processes on the unit sphere with locality and symmetry under azimuthal rotations, any distribution with support on a single meridian for each parallel would be considered as a "delta function along azimuthal rotations". In such a setting one may consider a further generalization of the data generation process, going beyond a single "delta function along  $\rho$ ". We leave these generalizations to future work.

 $<sup>^{13}</sup>d\tau$  can be thought of as the Haar measure on the 1-dimensional Lie group, but we do not lose much by treating the 1-dimensional Lie group under consideration to be the real numbers; for higher-dimensional, possibly nonabelian Lie groups, one will have to be more careful

#### 3.2 Architecture

Our model will start with a dataset  $\mathbf{X}$ , an  $N \times d$  matrix where N is the number of samples, and d is the dimensionality, and will learn an underlying symmetry group action  $\rho(\tau)$  and a local filter  $\psi^{(\mathbf{0})}$ . We will assume that the symmetry action  $\rho(\tau)$  is a real, unitary (i.e., orthogonal) representation, in other words, for each  $\tau$ ,  $\rho(\tau)$  will be a  $d \times d$  orthogonal matrix. We will also assume that the local filter (the "**resolving filter**")  $\psi^{(\mathbf{0})}$  acts by an inner product i.e.,  $\psi^{(\mathbf{0})}$  itself will be given by a d-dimensional (column) vector. While the underlying symmetry action  $\rho(\tau)$  will be a 1-dimensional Lie group action parametrized by the continuous parameter  $\tau$ , we will learn a "minimal **generator**"  $\mathfrak G$  of this action appropriate for the dataset at hand. This will be a generalization of the pixel translation operator for images.

Following the approach sketched in the introduction, for a given a candidate generator  $\mathfrak G$  and filter  $\psi^{(0)}$ , we will form an alternative representation  $\mathbf y$  for each d-dimensional sample vector  $\mathbf x$  by using a procedure analogous to a CNN: we will apply the filter  $\psi^{(0)}$  to transformed versions of  $\mathbf x$  under various powers of the generator  $\mathfrak G$ . In other words, for each sample (column) vector  $\mathbf x$ , we will have an alternative representation  $\mathbf y$  consisting of the components  $y_p = \psi^{(0)}(\mathfrak G^p(\mathbf x))$  where the power p will be  $0, \pm 1, \pm 2, \ldots$ 

These scalar representations of the samples will be our fundamental quantities on which we will apply the requirements of stationarity and locality. In the  ${\bf y}$  representation, the action by the generator  ${\mathfrak G}$  is represented by a simple shift of p, and thus if  ${\mathfrak G}$  is indeed a symmetry generator, the joint distribution of the scalars  $y_p$  should be invariant under shifts of p:  $p \to p + n$  (stationarity). Similarly,  $y_p$  and  $y_{p'}$  should be similar/strongly dependent as random variables if p and p' are close, and should be approximately independent otherwise (locality).

While there is no a priori restriction on the range of powers p to use in the representation, in this paper, we choose the same dimensionality of the representation y to be the same as the dimensionality of x. <sup>14</sup> More explicitly, for a given  $\mathfrak{G}$  and  $\psi^{(0)}$ , we we will form the  $d \times d$  matrix L, which we call the group convolution matrix, by

$$L = \begin{bmatrix} \begin{pmatrix} \mathbf{g}^{P_{min}} \end{pmatrix}^T \psi^{(\mathbf{0})} & \dots & \psi^{(\mathbf{0})} & \dots & (\mathbf{g}^{P_{max}})^T \psi^{(\mathbf{0})} \end{bmatrix}$$
 (5)

where  $P_{min}$  and  $P_{max}$  denote the minimum and maximum powers of the generator to be used. In our experiments we work with odd d, and pick  $P_{max} = \frac{d-1}{2} = -P_{min}$ . This matrix will be used to create a transformed version of the dataset  $\mathbf{X}$  via  $\mathbf{Y} = \mathbf{X}L$ . By using an appropriate loss on the resulting  $\mathbf{y}$  vectors, we will learn the  $\mathfrak{G}$  and  $\psi^{(0)}$  that have the needed locality and stationarity properties for the dataset  $\mathbf{X}$ .

Next, we describe the details of the model architecture, the loss function, and the technical choices made to learn the best  $\mathfrak{G}$  and  $\psi^{(0)}$  using the transformation L.

# 3.3 The generator and the filter

In order to learn an orthogonal matrix for  $\mathfrak G$  by design, we use the fact that any element  $\mathfrak G$  in the identity component SO(d) of the group O(d) of orthogonal matrices can be obtained by using the exponential map on an element of the Lie algebra of O(d), which is the algebra of  $d \times d$  antisymmetric matrices. Thus, we will learn a  $d \times d$  matrix A to determine  $\mathfrak G$  via 15

$$\mathfrak{G} = \operatorname{Exp}\left(\frac{A - A^T}{2}\right) \tag{6}$$

where the matrix exponential can be defined in terms of the Taylor series.

While the resolving filter  $\psi^{(0)}$  is learned without constraints, we will use a normalized version of it in our computations of the group covariance matrix L.

#### 3.4 The loss function

Our loss function will act on the transformed version  $\mathbf{Y} = L\mathbf{X}$  of each batch  $\mathbf{X}$  of data to ensure the stationarity (uniformity) and the locality properties. The building blocks of the loss function involve the correlation between the successive components of a transformed sample vector  $\mathbf{y}$ , entropy estimates for the components of this vector, and KL divergences between estimated densities for components. We first describe the pieces of the loss function assuming one has access to estimates of the necessary quantities like entropy and density, and will then explain the techniques used for estimating these quantities for each batch.

 $<sup>^{14}</sup>$ Our methodology does not rely on this choice, and one could easily consider other ranges for p.

<sup>&</sup>lt;sup>15</sup>To optimize memory usage, one could use a more efficient parametrization of antisymmetric matrices

#### 3.4.1 Stationarity/uniformity

If the learned group convolution matrix L indeed corresponds to an underlying symmetry, we expect the joint distribution of the components of  $\mathbf{y}$  to be invariant under shifts of its components (modulo boundary effects). Since computing the joint probability density is impractical in high dimensions, we instead compute a proxy for this expected symmetry in terms of the distributions of individual components and pairs of components. More explicitly, for each component pair  $(y_i, y_j)$  of the learned representation, we compute the KL divergence between the estimated densities of  $(y_i, y_j)$  and  $(y_{i+1}, y_{j+1})$  and our loss is a sum of the averages of these KL divergences.

If we have estimates of the joint probability densities  $\hat{f}_{ij}$ ,  $\hat{f}_{kl}$  for components  $y_i, y_j$  and  $y_k, y_l$ , respectively, the KL divergence  $D_{KL}(f_{ij}, f_{kl})$  between them can be approximated by

$$D_{KL}(f_{ij} \parallel f_{kl}) \approx \hat{D}_{ij;kl} = \mathbb{E}\left[\hat{f}_{ij}(y_{ij})\log\hat{f}_{kl}(y_{ij})\right]$$
(7)

where the expectation  $\mathbb{E}$  is computed as an average over all the samples in a batch of data used during optimization. Our uniformity loss is given by

$$\mathcal{L}_{uniformity} = \left\langle \hat{D}_{ij;i-1,j-1} \right\rangle_{\substack{1 \le i < d \\ 1 \le j < d \\ j \ne i}} + \left\langle \hat{D}_{ij;i+1,j+1} \right\rangle_{\substack{0 \le i < d-1 \\ 0 \le j < d-1 \\ j \ne i}}$$
(8)

This loss function forces the relationships between pairs of components to be symmetric under shifts of components. We find that this second order proxy to the symmetry of the joint distribution both results in highly stable behavior, and is computationally tractable.

# 3.4.2 Locality

Our locality loss consists of two pieces that we call alignment and resolution. Alignment loss aims to make neighboring pixels have similar information, and resolution aims to make far away pixels have distinct information.

**Alignment** The correlation between two real-valued random variables gives a measure of the linear dependency between them. We would like successive components of y to not only have similar distributions (as in the uniformity loss), but to have similar values in each sample. Thus, we use the correlation coefficient between successive components as part of our locality loss.

For each batch of data, we compute the Pearson correlation coefficient  $\rho_{i,i+1} \in \mathbb{R}$  of the components  $y_i$  and  $y_{i+1}$  of y, and define the alignment loss  $\mathcal{L}_{alignment}$  as the average of this quantity over all successive pairs of components

$$\mathcal{L}_{alignment} = -\langle \rho_{i,i+1} \rangle_{0 < i < d-1} \tag{9}$$

**Resolution** We would like to have a quantity that forces the components  $y_i$  and  $y_j$  of y to contain distinct information when i and j are not close. One proxy measure for this can be obtained by considering the amount of Shannon information in the whole vector y, and the information in its individual components. In the information theory literature, the quantity

$$C(\mathbf{y}) = \sum_{i=1}^{d} h(y_i) - h(\mathbf{y})$$
(10)

called the *total correlation*, measures the degree to which there is shared information between the components of  $\mathbf{y}$ . In our setting, since only nearby components should share information (which is enforced by the alignment loss above), and all other pairs of components should be approximately independent, we expect  $C(\mathbf{y})$  to be small. We thus use an approximation to  $C(\mathbf{y})$  over each batch as our resolution loss.

As we describe in our discussion 3.6.2 on optimization below, we perform our entropy estimates  $k \times \bar{h}_k(\mathbf{y}) \approx h(\mathbf{y})$  by using an epoch-dependent rank k for a relevant covariance matrix. In effect, this increases the number of variables that to into the entropy estimate from k=1 to k=d over the course of the estimation. To use a stable measure for the resolution loss, we thus use a normalization on  $C(\mathbf{y})$  to define

$$\mathcal{L}_{resolution} = \frac{1}{d} \sum_{i=1}^{d} h(y_i) - \bar{h}_k(\mathbf{y})$$
(11)

which is computed for each batch.

<sup>&</sup>lt;sup>16</sup>In the implementation, we split joint probability to marginal probability and conditional probability to have a finer grain of control over the experiments.

#### 3.4.3 Information preservation

While the "correct directions" in parameter space (i.e., directions that get us close to an actual symmetry generator and a local filter) reduce the locality and uniformity loss terms described above, there is also a simple, catastrophic solution for the map L that can minimize these terms, namely, projecting the data to a single point. Indeed, we would like to learn a transformation that has symmetry and locality properties, but we also want this transformation to preserve the information content of the data.

For this purpose, we add a final term to our loss function that aims to maximize the mutual information between the input x and the output y. For a deterministic map, this mutual information can be maximized by simply maximizing the entropy of the output (see C for a proof, and the InfoMax principle proposed in [23]). As mentioned above and as will be further explained in our section 3.6.2 on optimization considertaions, our entropy estimate will use an epoch-dependent "rank" k, and we use this estimate in our entropy preservation loss:

$$L_{preservation} = -\bar{h}_k(\mathbf{Y}) \tag{12}$$

#### 3.4.4 Total loss

Merging the overall loss terms we have

$$\mathcal{L} = \alpha \mathcal{L}_{alignment} + \beta \mathcal{L}_{resolution} + \gamma \mathcal{L}_{uniformity} + \delta \mathcal{L}_{preservation}$$
 (13)

while  $\alpha, \beta, \gamma, \delta \in \mathbb{R}$ . After limited experimentation, we fixed the hyperparameters to 1.5, 1.5, 2.5, 2.5, respectively and used the same values in all our experiments.

#### 3.5 Estimators

As mentioned above, to compute the loss (13), we need to have estimates of various probability densities and entropies. These estimators have their own loss functions and optimization, which we summarize here. For details, see the appendix.

# 3.5.1 Multidimensional entropy estimation

To estimate the multidimensional differential entropy of the transformed data y, we use a multivariate Gaussian approximation to the distribution of y. In addition to being computationally efficient, this approach also allows us to use a dynamic approach to entropy estimation by using an epoch-dependent choice for the rank of the Gaussian, as explained in section 3.6.2.

For each batch of size N, we start by centering components of  $\mathbf{y}$  so that  $\sum_{n=1}^{N} y_{ni} = 0$  for each  $i \in [1, d]$ , and we compute an approximation  $\mathbf{C} = (c_{ij}) \in \mathbb{R}^{d \times d}$  to the covariance matrix via

$$cov(y_i, y_j) = \mathbb{E}[y_i y_j] \approx c_{ij} = \frac{1}{N} \sum_{i=1}^{N} y_{ni} y_{nj}$$
(14)

Under the multivariate Gaussian assumption, the total entropy of a distribution with a given covariance matrix can be written as the sum of the entropies of its principal components, i.e., if  $\lambda_i$  denotes the eigenvalues of the matrix  $\mathbf{C}$ , then  $h(\mathbf{y}) = \sum_i h_i$  where

$$h_i = \log(\lambda_i) \tag{15}$$

We assume the eigenvalues are sorted according to their magnitudes so that  $h_i$  is the entropy of the principal component having the i'th highest variance.

For purposes of efficient optimization as described in Section 3.6.2, we also define a rank-k approximation to the entropy. This consists of a weighted average of the per component contributions to entropy

$$\bar{h}_k \triangleq \frac{\sum_{i=1}^d w_{ki} h_i}{\sum_{i=1}^d w_{ki}} \tag{16}$$

where the weights provide a soft thresholding at  $\boldsymbol{k}$  via

$$w_{ki} = \frac{1}{e^{\alpha(i-k)} + 1} \tag{17}$$

where  $\alpha$  is a hyperparameter. Our experiments have shown that the results are stable for different choices of  $\alpha > 1$ .

Note that (16) should be thought of as a "per-rank" version of low rank entropy, due to the denominator. In particular, when comparing it to the marginal entropies of each component  $y_i$  of y, it is more appropriate to compare it to average marginal entropy rather than the total marginal entropy.

#### 3.5.2 Probability density estimation

For estimating probability densities, we use the mixture of Gaussians approach described in [24]. This estimator is trained by using stochastic gradient descent-based optimizers such as ADAM to minimize the entropy of estimated probability densities. For further details, see A

# 3.6 Training the model

#### 3.6.1 The training loop

Our system is composed of two separate subsystems with different training objectives, loss functions, and optimizers. One subsystem seeks the generator  $\mathfrak G$  of symmetries and the resolving filter  $\psi^{(0)}$ . We train this subsystem with the loss term described above involving locality, uniformity, and information preservation terms. The second subsystem is made up of probability estimators. These estimators are trained to minimize their output entropy as described in [24]. The training for the two subsystems is done jointly, with simultaneous gradient updates.

#### 3.6.2 Optimization considerations

Controlling the rank of the joint entropy During our experiments, we observed that when the total entropy term in the loss function was computed naively, it dominated the training dynamics from the beginning and resulted in the optimizer getting stuck in local minima. Inspired by iterative optimization processes such as normalizing flows[?], we developed a special regularization procedure to solve this problem. The main idea is to use a low-rank estimate of the entropy at the beginning, and to gradually increase the rank of the estimation during optimization. This is achieved by using a dynamic weighting of the entropies of each principal component in succession so that the information content of the most informant (biggest variance) component is maximized early in the training, and less informant (lower variance) principal components are added later. This allows a more effective traversal of the loss function landscape.

To choose the dynamic weights, we use a normalized notion of training time  $t_n$ , which measures the "amount of gradient flow". We define  $t_n$  as

$$t_n = \frac{\sum_{s=1}^{n} \ln(s)}{\sum_{s=1}^{T} \ln(s)}$$
 (18)

where lr(s) is the learning rate used at training step (batch) s, and n and T are the current and the total training steps, respectively.

Given this notion of time, we control the rank k of the low-rank entropy estimator via

$$k = \operatorname{ceil}(d \times t_n) \tag{19}$$

so that by the end of the training, the rank is at d.

Noise injection to the resolution filter In order to avoid an initialization-based bias in the optimization, we initialize the resolving filter with zeros and add Gaussian noise during the early stages of training before computing the loss for each batch. The amplitude of the noise is set to decay exponentially with a short time constant (of  $\tau=10$  epochs), which was sufficient:

$$\tilde{\psi}^{(0)} \leftarrow \psi^{(0)} + \mathcal{N}(\mu = 0, \sigma = 0.1) \exp(-(t/\tau))$$
 (20)

As mentioned previously, to compute the transformed data y, we use a normalized version of  $\psi^{(0)}$  at each step:

$$\hat{\psi}^{(\mathbf{0})} = \frac{\tilde{\psi}^{(\mathbf{0})}}{||\tilde{\psi}^{(\mathbf{0})}||_2} \tag{21}$$

**Padding** We use a "padding" for the symmetry generator and the filter in the sense that the symmetry matrix and the filter have dimensionality that is higher than the dimensionality of the data, but we centrally crop the matrix and the filter before applying them to the data. This is done to deal with edge effects, and after experimenting with padding sizes for 6 to 33, we saw that the results are not sensitive to padding size. We will expand on the padding and the case of circulant symmetries in a future draft of the paper.

**Initialization of the symmetry generator** We initialize the matrix A used to obtain the symmetry generator  $\mathfrak G$  using a normal distribution with  $\sigma=1e-3$  and  $\mu=0$ . This leads to an approximate identity for the generator  $\mathfrak G$  via the exponential map. Using smaller standard deviations did not affect performance, however, significantly larger sigma values may lead to learning a higher power of the underlying symmetry generator instead of learning the minimal generator.

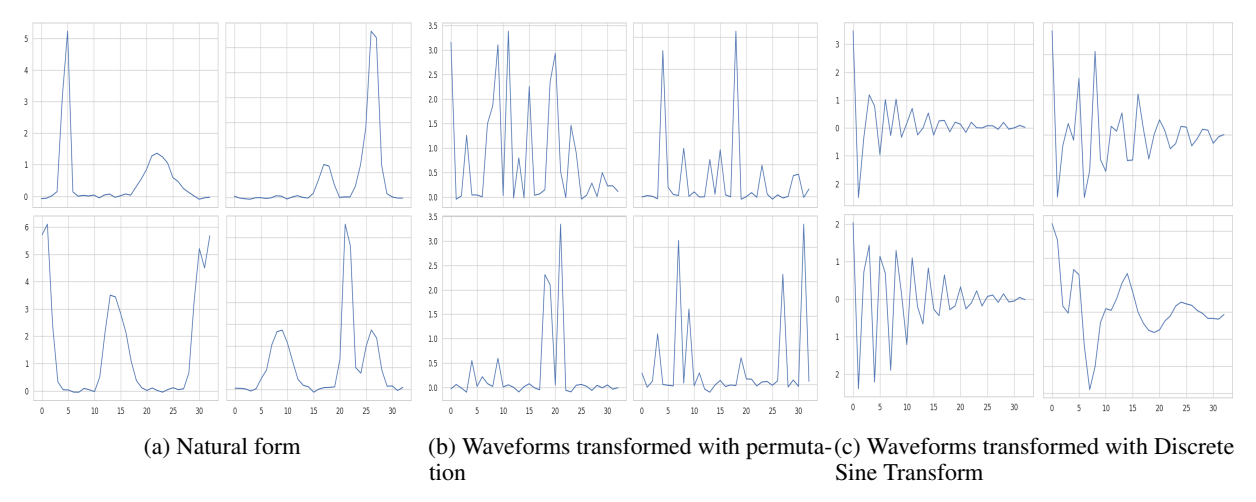


Figure 6: Signal samples built from Gaussian basis functions. In each figure, the x-axis represents the component index (or the "pixel index") of the sample vectors, and the y-axis is the amplitude of the corresponding component. Each signal shown consists of a number of Gaussian bumps with random centers and widths in some symmetry space, together with some noise. In (a), we show signals that are "spatially localized", with a distribution that is invariant under spatial shifts. In other words, the symmetry generator in this case shifts the components ("pixels") of the signal by one unit. The signals in (b) have a locality/symmetry that maps each component ("pixel") of the signal to another component, but using a different ordering, e.g. the symmetry generator is something like Pixel  $1 \rightarrow \text{Pixel } 17 \rightarrow \text{Pixel } 3$ , etc. Although these examples have a locality and symmetry just as in (a), this is not apparent to the naked eye, but the model is able to discover this just as it can discover simple pixel translations. In (c), the signals are local/symmetric along the "frequency axis". In other words, each signal consists of a few Gaussian bumps in Fourier space (we use Discrete Sine Transform I), and the dataset as a whole is symmetric under shifts of the frequencies, while in each sample, the "excitations" are local in frequency space. While these examples show some regularity, it is not clear at all visually that there is a precise locality/symmetry in frequency space. The model is able to decipher this symmetry, as well.

# 4 Data

We use synthetically generated datasets to train the models. Our datasets have symmetry (stationarity) and locality properties along various symmetry actions. The data generation procedure is as follows.

- 1. Each dataset is built from a type of "local basis signal" such as a Gaussian.
- 2. We use a Binomial distribution with probability p=0.5 and n=5 to determine the number of "component signals" to include in each sample.
- 3. To obtain each component signal, we sample the parameters of the basis signal such as its center, width, and amplitude from uniform distributions. <sup>17</sup>
- 4. We add up the component signals to get a sample with locality under simple pixel translations (i.e., shifts of the components of the vector).
- 5. According to the chosen symmetry representation, we apply a unitary transformation to the sample to get locality/symmetry in the desired direction.
- 6. We add noise to the samples to mimic realistic conditions.

Each sample will be a 33-dimensional vector, in other words, the basis signals will have a discrete x-axis, consisting of 33 components. See Figures 6, 7 for some examples.

The symmetry actions that we consider are as follows.

**Pixel translations.** This is the symmetry of the original samples that we create, before applying any unitary transformation, examples are shown in Figures 6, 7. In these datasets, the dimensions of the samples can be thought of as pixel indices in 1-dimensional image data, and each "image" consists of a few local bumps whose center pixel indices are random.

<sup>&</sup>lt;sup>17</sup>Experiments with nonuniform distributions resulted in similar behavior.

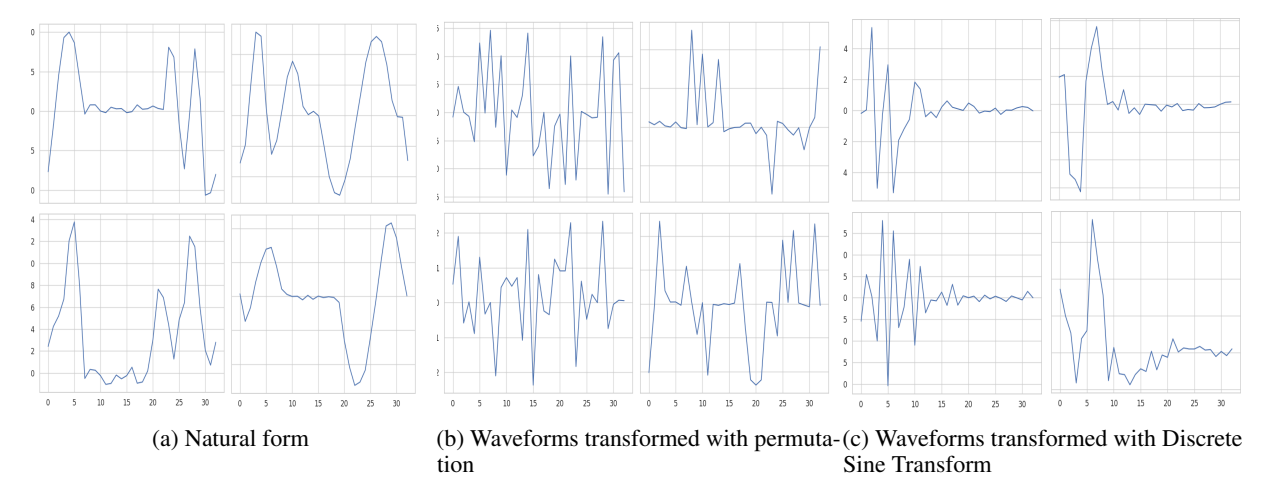


Figure 7: Signal samples built from Legendre basis functions. Analogous to Figure 6, but using Legendre functions as basis functions instead of Gaussians, as described in the text.

**Powers of a fixed permutation of components.** In this case, we start with a dataset symmetric under pixel translations, and apply a fixed permutation to the components of each sample. The resulting dataset will be local and symmetric under the group generated by the powers of a new permutation. As a simple example, consider a 4-dimensional dataset and the fixed permutation P that swaps pairs of components  $x_1 \leftrightarrow x_2, x_3 \leftrightarrow x_4$ :

$$P = \begin{bmatrix} 0 & 1 & 0 & 0 \\ 1 & 0 & 0 & 0 \\ 0 & 0 & 0 & 1 \\ 0 & 0 & 1 & 0 \end{bmatrix}$$
 (22)

While the original samples x will be symmetric under shifts of the components  $x_1 \to x_2 \to x_3 \to x_4$ , the components of the transformed version y will be given via

$$\begin{bmatrix} y_1 \\ y_2 \\ y_3 \\ y_4 \end{bmatrix} = \mathbf{y} = P\mathbf{x} = \begin{bmatrix} x_2 \\ x_1 \\ x_4 \\ x_3 \end{bmatrix}$$
 (23)

and will be invariant under  $y_2 \to y_1 \to y_4 \to y_3$ . More generally, The symmetry generator of the new dataset will be given by  $P \cdot T \cdot P^{-1}$  where T denotes the simple pixel shift operator. Note that starting with a simple dataset with pixel locality/symmetry, this results in a dataset with a highly obscured symmetry like Pixel  $1 \to Pixel 17 \to Pixel 5 \to etc.$ 

Frequency shifts. In this case, the dataset will be symmetric/local under shifts of frequencies. More explicitly, we would like to consider a dataset that is invariant under the shifts of the components of its discrete sine transform, i.e., a transform that takes the amplitude of the lowest frequency component and makes it the amplitude of the second frequency, etc. To get a dataset that is local/invariant under such a transformation, we apply the inverse  $D^{-1}$  of the discrete sine transform D to the "pixel translations" dataset. This results in the generator  $D^{-1} \cdot T \cdot D$ , which simply shifts the frequencies as desired.

**Dispersion shifts.** We will describe this in a future draft.

## 4.1 Basis signal types

**Gaussian signals** Gaussian signals are parametrized by amplitude A, mean  $\mu$  and standart deviation  $\sigma$ 

$$f_{gaussian}(x; \mathcal{A}, \mu, \sigma) = \frac{\mathcal{A}}{\sigma\sqrt{2\pi}} \exp\left(-\frac{(x-\mu)^2}{2\sigma^2}\right).$$
 (24)

where x becomes the dimension index in the dataset.

<sup>&</sup>lt;sup>18</sup>The edge effects can be dealt with by using cyclic translations of pixels in the original dataset, or by using a padding.

**Legendre signals** These signals are given in terms of the associated Legendre polynomials and give localized waveforms that can change signs. These functions are parametrized by their center c, scale s and amplitude A:

$$f_{legendre}^{(l,m)}(x; \mathcal{A}, c, s) = \begin{cases} \mathcal{A}P_l^m\left(\cos\left(\frac{x-c}{s}\right)\right) &, |x-c| \le s\\ 0 &, \text{otherwise} \end{cases}$$
 (25)

where once again x becomes the dimension index. For this set of basis signals, we crop the signal to between  $-\pi \le (x-c)/s \le \pi$ , in the sense that we set all values for x outside this range to zero. For the l,m parameters, we use l=2, m=1 and l=3, m=1.

#### 4.2 Output transformation

As described above, given a dataset  $\tilde{\mathbf{X}}$  with simple translation symmetry (of shifting its dimensions, or pixels), we apply additional unitary transformations to change the symmetry behavior:

$$\mathbf{X} = \tilde{\mathbf{X}}\mathbf{U} \tag{26}$$

where **X** is the final,  $N \times d$  dataset with the desired symmetry, and **U** is the  $d \times d$  unitary transformation that changes the symmetry action. The set of transformations we use are <sup>19</sup>

- Identity (no transformation)
- Random permutation
- Discrete sine transformation of type I

# 4.3 Prepared datasets

We prepared nine synthetic datasets whose properties are given in Table 1. The parameters for each basis signal are sampled from a uniform distribution with the indicated ranges. For all datasets, we added Gaussian noise with  $\sigma = 0.05$ .

Signal Type	Transformation	Amplitude	Scale		
		range	range		
Gaussian	Identity	[0.5, 1.5)	[0.5, 2.5)		
Gaussian	Permutation	[0.5, 1.5)	[0.5, 2.5)		
Gaussian	DST-I	[0.5, 1.5)	[0.5, 2.5)		
Legendre(l=2-3,m=1)	Identity	[0.5, 1.5)	[6.0, 15.0)		
Legendre(l=2-3,m=1)	Permutation	[0.5, 1.5)	[6.0, 15.0)		
Legendre(l=2-3,m=1)	DST-I	[0.5, 1.5)	[6.0, 15.0)		

Table 1: Synthetic dataset properties

# 5 Results

# 5.1 Model performance and behavior

For each dataset listed in 1, our model was trained to learn the ingredients of the symmetry group convolution map L, i.e. the group action generator  $\mathfrak G$  and the resolving filter  $\psi^{(0)}$ . The group generator  $\mathfrak G$  has a known, correct answer in this case, which was, of course not given to the model in any way—the model was to learn the symmetry generator in an unsupervised way. Each model was trained for  $10\mathrm{K}$  epochs.

A visual description of outcomes of the experiments are given in Figures 8, 9, 10, 11, 12, 13, 14, 15 and here we give a summary:

- The symmetry generator  $\mathfrak G$  learned in each case is indeed approximately equal to the underlying, correct generator used in preparing the dataset. See Figures 8, 9, 10.
- The group convolution operator L formed by combining the learned generator  $\mathfrak{G}$  with the learned resolving filter  $\psi^{(0)}$  in each case is approximately equal to the underlying transformation used in generating the dataset. See Figures 11, 12, 13.

<sup>&</sup>lt;sup>19</sup>We will describe the dispersive transformation in a future draft.

- The learned group convolution operator is highly successful in reconstructing the underlying hidden, local signals. See Figures 14, 15.
- The same hyperparameters have been used in each case—all the settings including the learning rates, low-rank entropy estimation scheduling, batch size, etc., were the same for all experiments. In other words, no fine tuning was necessary for different data types.
- The results are stable in the sense that training the system from scratch results in similar outputs each time.

Some notable properties of the method worth emphasizing are as follows.

**Learning the minimal group generator.** A dataset with a pixel translation symmetry also has a symmetry under two-pixel translations, three-pixel translations, etc. In fact, each one of these actions could be considered as a generator of a subgroup of the underlying group of symmetries. Some works in the literature have successfully learned symmetry generators from datasets, but ended up learning one of many subgroup generators instead of the minimal generator. Our inclusion of locality together with stationarity in the form of alignment and resolution losses has allowed the method to learn the minimal generator in each case.

**Accuracy.** We compute root mean squared error and the true cosine similarity between the learned symmetry generator and the true, underlying generator.<sup>20</sup> The results are are shown in 2, and the error plots are in Figures 8, 9, 10. We see that the accuracy is stable across different datasets, and most of the small error is due to edge effects.

Strength against the curse of dimensionality. The dimensions of the datasets we use (d=33) is higher than many of the works that have a comparable aim to ours (i.e. unsupervised learning of symmetries from raw data [4, 15, 16]). In a 33-dimensional dataset, the search space of symmetry operators is large, and getting stuck in local minima, finding spurious symmetries, etc., are common problems (which we, indeed, also had to battle with in previous iterations of this work). Our approach to the loss function involving locality, stationarity, and information preservation, has resulted in a highly robust system that reliably finds the correct symmetries in each of the examples we tried. Moreover, the system is nowhere near its limit in terms of dimensionality; our initial experiments with twice the dimensionality gave similar preliminary results. We are implementing some computational optimizations to further scale the system.

**Robustness against noise.** While the underlying symmetry for each data generation procedure was exact, the datasets were only approximately symmetric (due to random sampling of centers and widths, etc.), and moreover random nois was added to each sample. Thus, the search was symmetry had to be robust. Our coupling of information-theoretic metrics to a simple correlation loss for nearby pixels has enabled the necessary robustness against noise.

**Fixed hyperparameters for all experiments.** We did not need to tune the hyperparameters separately for each dataset, one setting obtained by limited experimentation on a dataset worked equally well for all our datasets. This, too is a sign of the stability of the system.

An adaptor between CNNs and raw data with unknown symmetry. Since the method is able to learn a minimal generator of the underlying symmetry, together with a resolving filter that is "tight" along the symmetry direction, it has been able to recover a version of the data that is symmetric simply under the shifts of components. Now, such a representation is exactly the type of situation where CNNs are effective. Thus, for a given supervised learning problem, say, one can fist train our model to learn the underlying symmetry, and then transform the data with the resulting group convolution layer, and then feed the resulting representation to a multi-layer CNN architecture.

The resolving filter. In addition to the symmetry generator, our model learns a resolving filter that is local along the symmetry direction. While we have not explicitly forced the model for this, in each case, the learned resolving filter was an approximate "delta function along the symmetry direction" as described in Section 3.1. In the case of simple translation symmetry, the filter has a single nonzero component, in the case of the frequency shift, it is a pure sinusoidal. This behavior is simply a consequence of the loss function we use that couples locality and symmetry in a particular way: the filter that satisfies the required properties to the highest degree is a highly local filter in the symmetry direction.

**Signal reconstruction.** When we apply the group convolution operator obtained by combining the resolving filter with the powers of the symmetry generator, we get a representation of the data along the symmetry directions. This representation was forced to be local and symmetric by our loss function, but due to the behavior of the learned resolving

<sup>&</sup>lt;sup>20</sup>Cosine similarity here is obtained by treating the generator matrix as a vector, or, equivalently, using the Hilbert-Schmidt (or Frobenius) inner product between the two matrices.

TC 1 1 2 T 1		1 .			
Table 2: Learned	generators	compared to	1deal	mınımal	generators

Symmetry	Gaussian dataset	Legendre dataset	
Translation	Cosine similarity : 0.996 RMSE : 0.016	Cosine similarity : 0.997 RMSE : 0.014	
Permuted	Cosine similarity : 0.999 RMSE : 0.002	Cosine similarity : 0.998 RMSE : 0.010	
Frequency space	Cosine similarity : 0.988 RMSE : 0.027	Cosine similarity : 0.993 RMSE : 0.020	

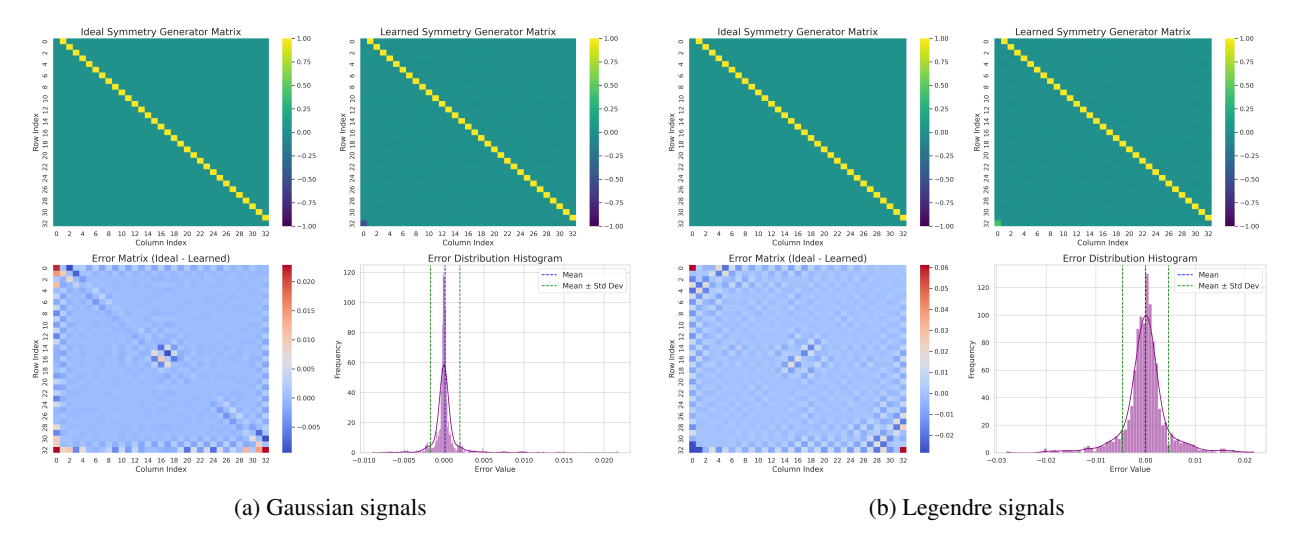


Figure 8: Comparisons of ideal and learned translation generators for Gaussian and Legendre datasets. For both datasets, we see that it's hard do discriminate the difference between the ideal symmetry generator and the learned one. We see that error increases, at the edges, which hints edge effects may be the source of current errors and the results can be further improved by increasing padding. Error is normally distributed for both of the datasets, indicating that error sources don't have systematic nature.

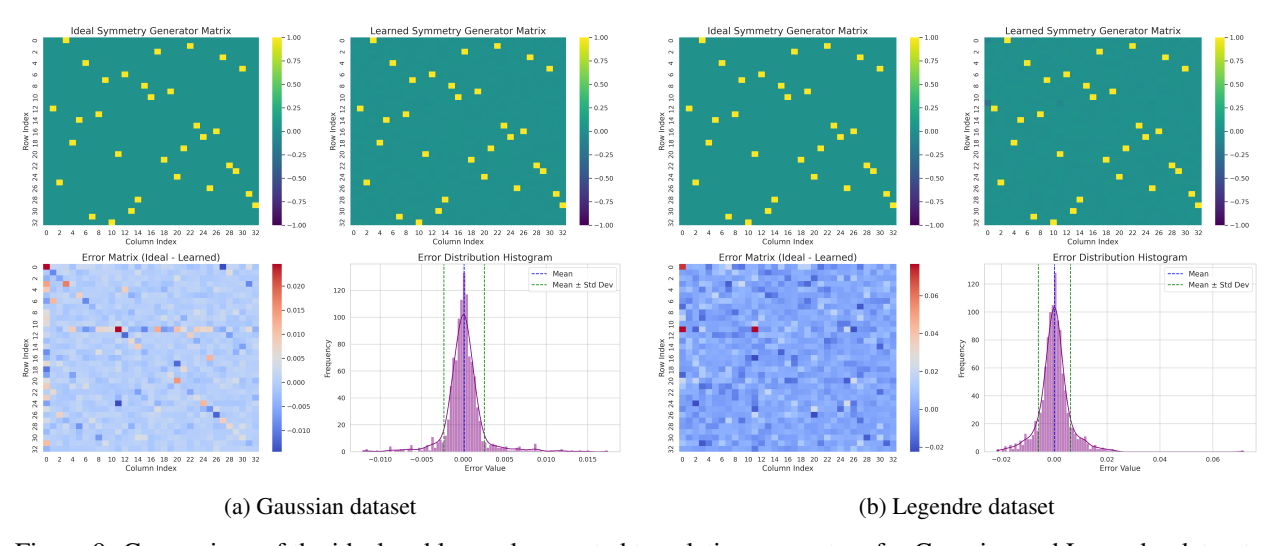


Figure 9: Comparison of the ideal and learned permuted translation generators for Gaussian and Legendre datasets. We see that error distribution is quite similar to the translation case validating bias-free nature of the method from a different perspective. However, in this case edge effects are invisible since shuffling mixes their positions.

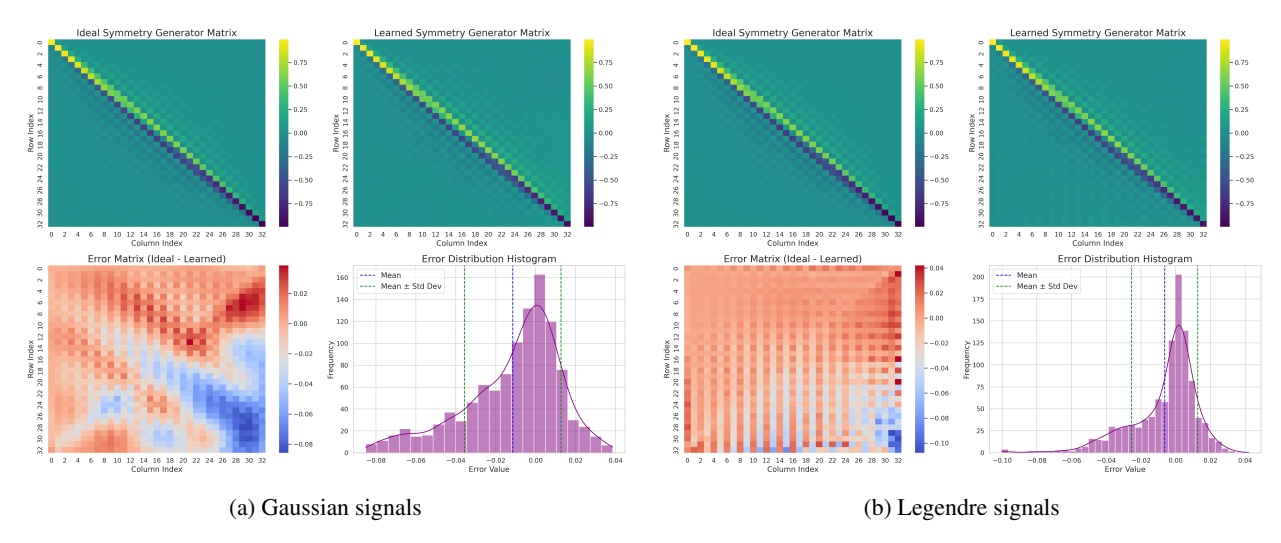


Figure 10: Comparison of the ideal and learned frequency domain translation generators. Although error margin is still small, we see that the error related to lower frequency components dominate which also leads to skewed distribution. We plan to evaluate this behavior further in the future to improve current performance metrics.

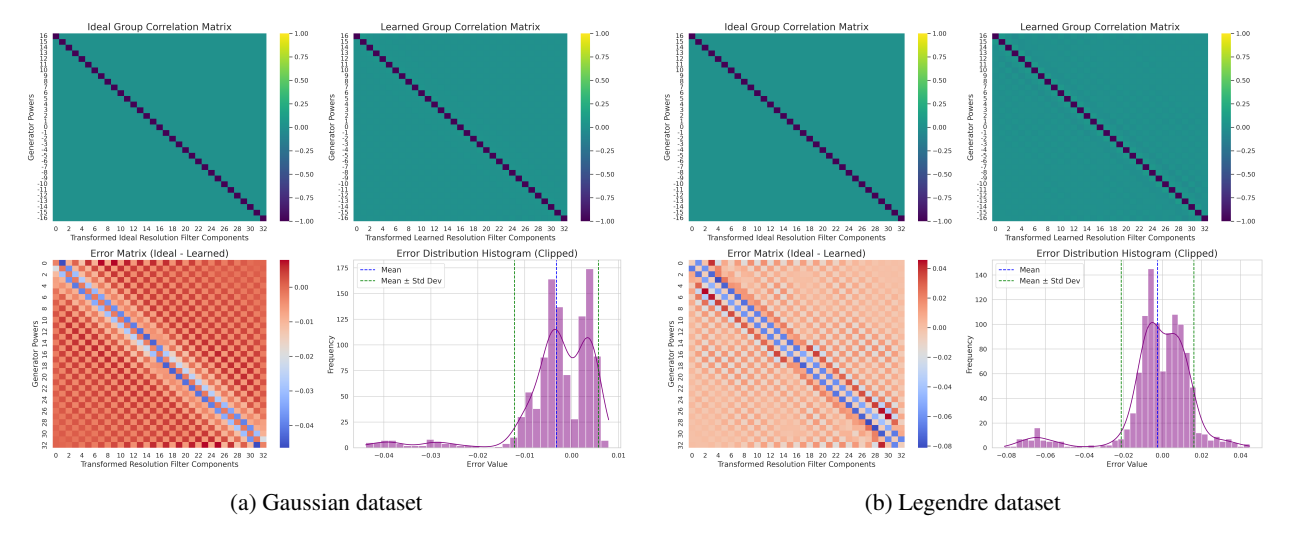


Figure 11: Comparison of ideal and learned group convolution maps for datasets with translation symmetry. We see that the model has learned identity operation upto a sign for both Gaussian and Legendre datasets, respecting the already present structure of the dataset. We observe that the error distribution shows the similar odd behavior for both of the datasets. However, it can be interpreted as mixture of two gaussian error distributions with different. This gaussian error distributions can be emerged due to errors of the symmetry generator for positive and negative powers.

filter described above, it actually does more. For the case of the 1-parameter datasets used in this paper, the output representations are almost equal to the hidden local representations, in other words, the model extracts the hidden local signal from the raw data almost perfectly.

## 5.2 Training dynamics

To investigate the training dynamics of the models we took snapshots of the symmetry generator and the group convolution matrices. We see that during the course of training, optimization paths are similar and repeatable along different experiments. In Figure 16, we show snapshots of the group generator for the simple "pixel" translation symmetry and the frequency shift symmetry. Similarly, in Figure 17, we show snapshots of the group convolution matrices. We find the gradual appearance of (effectively) the Discrete Sine Transform matrix as the group convolution

<sup>&</sup>lt;sup>1</sup>To simplify interpretation, we invert the model's output or flip its sign when necessary.

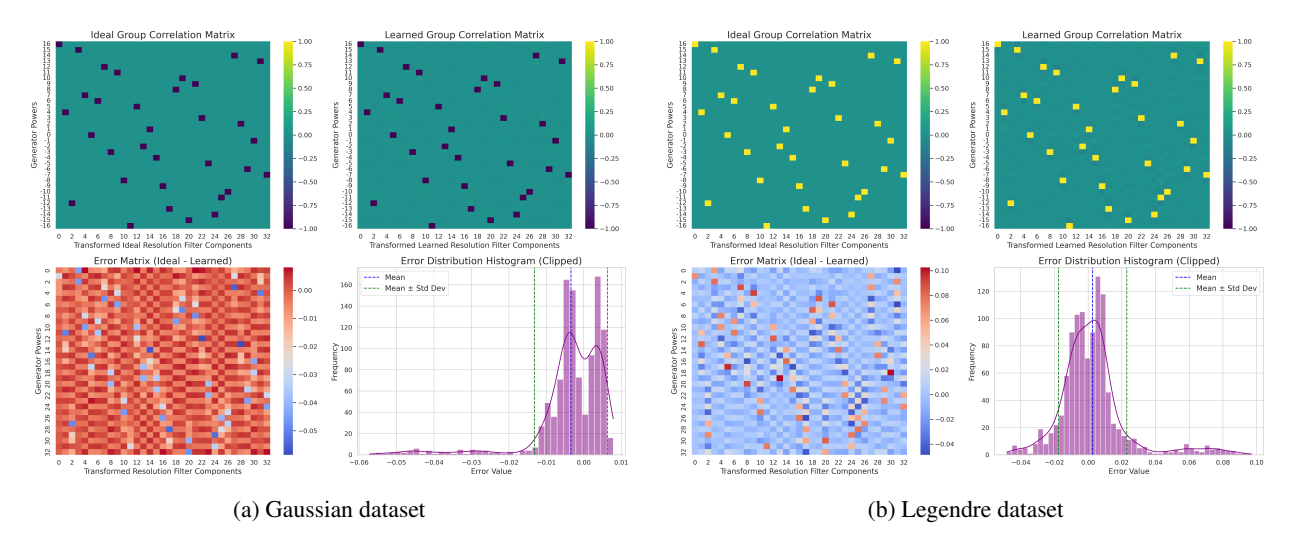


Figure 12: Comparison of ideal and learned group convolution matrix for datasets with permuted translational symmetry. We see that the model has learned a permutation, which reveals itself when we investigate it's output. However, this time, group convolution matrix doesn't flip the sign for Legendre dataset while it flips it in Gaussian dataset. This behavior shows itself since the method only depends on the intrinsic properties of the underlying representations. Error distributions are similar to the component translation case.

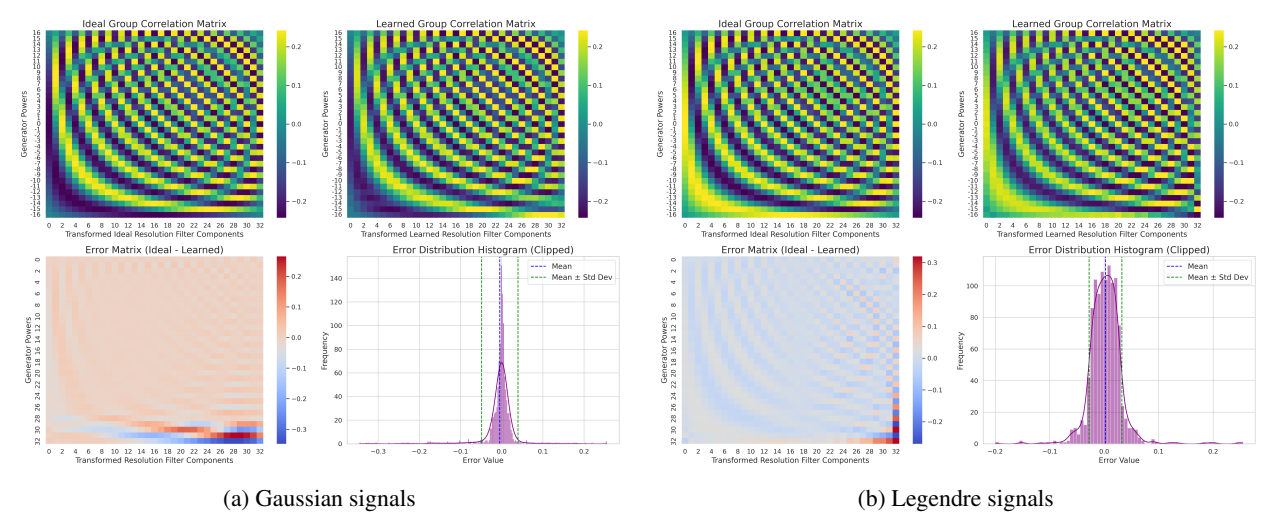


Figure 13: Comparison of ideal and learned group convolution maps for data with symmetry along frequency space. Surprisingly, we see that the model learns transposed Discrete Sine transformation Matrix of Type I. This negates the effect of using frequency space translation and maps this signal to the same representation as in the other symmetries. Error heatmaps imply that lower frequencies contribute to errors more significantly, which we plan to investigate further.

matrix particularly striking, though of course, learning the pixel translation matrix and the resulting group convolution (which is the identity matrix) is just as difficult a problem to solve, when the model is completely blind to the underlying data generation procedure.

The training dynamics is greatly facilitated by the low-rank entropy estimation procedure described in Section 3.6.2. By first extracting the gross behavior of the current maps and optimizing for that gross behavior, and only then increasing the resolution by using a higher-rank estimator and further improving the model, the training dynamics can have a much better chance of navigating the complex loss landscape.

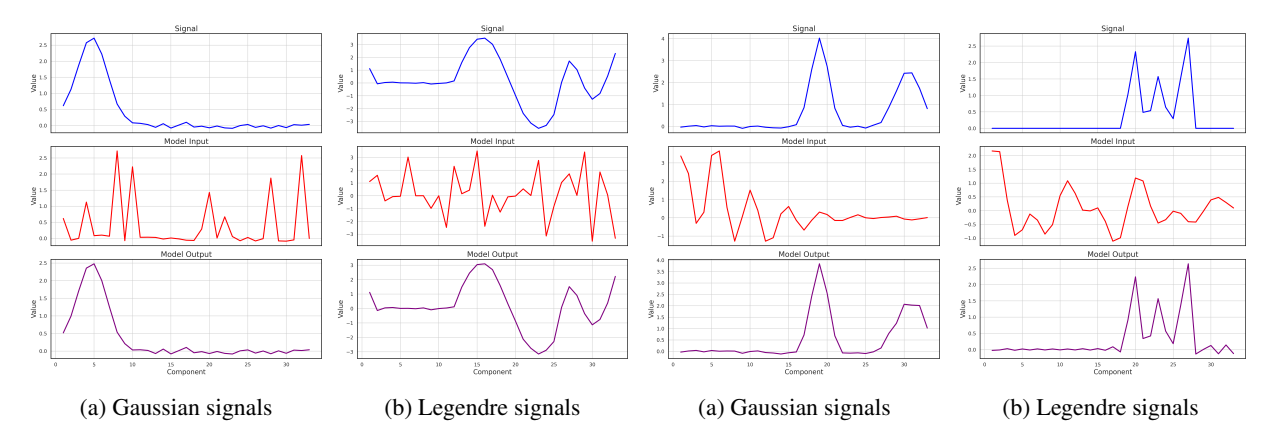


Figure 14: Hidden and revealed signals when permutation Figure 15: Hidden and revealed signals when Discrete Sine is applied during the data generation. For both of the Transformation is applied during the data generation. We datasets, we see that the effect of permutation is inverted see that locality in the frequency space is revealed and the leading to much more interpretable data while it's not signals are mapped to the natural representation.<sup>1</sup> possible to interpret by the naked-eye.<sup>1</sup>

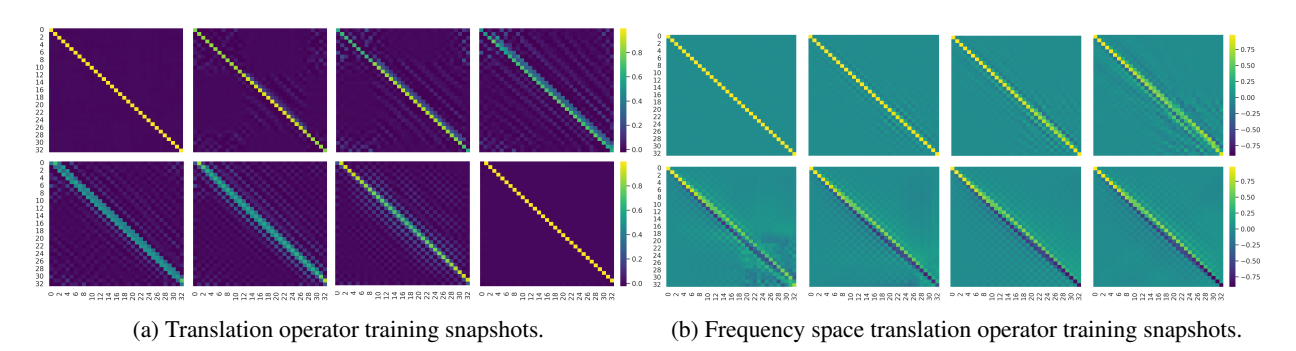
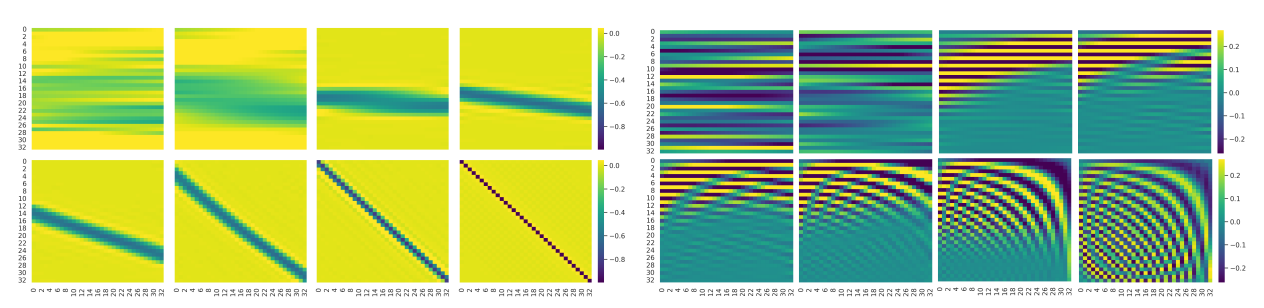


Figure 16: Snapshots taken during training on dataset involving various symmetries. We see that for all cases the generator starts at the identity and it evolves continuously through the minimal generator without losing track or showing chaotic behavior.



(a) Group convolution matrix training snapshots for translation-(b) Group convolution matrix training snapshots for frequency ally symmetric data.

Figure 17: Snapshots of the group convolution matrices taken during training on datasets with component and frequency space translation symmetry. Initially, all matrices are same along the rows axis which is due to the generator starting at identity. Since we form the group convolution matrix by stacking resolving filters acted with different powers of the group generator, all columns become similar. We observe that, training involves improving the rank of the group convolution matrix at initial phases. This is followed by learning finer details at the later phases of training.

# 6 Discussion

Our experiments show that the method described in this paper can uncover the symmetries (generators of group representations) of quite different sorts, starting with raw datasets that are only approximately local/symmetric under the action of a 1-dimensional Lie group. Moreover, the choice of the loss function and the approach used in optimization have resulted in highly stable and robust results. This is the outcome of extensive experimentation and detailed studies of various different approaches to the same intuitive ideas described in the introduction. It is satisfying, and perhaps not surprising, that the current, successful methodology is the simplest among the range of approaches we have previously tried.

In this paper, we focused on the action of a 1-dimensional Lie group, generalizing the pixel-translation symmetry of images in one direction. Natural images have 2-dimensional translation symmetries (along two orthogonal directions), and it would be satisfying to recover this symmetry, which, after all, the original symmetry of 2D CNNs. Our method can easily be generalized to two commuting symmetry generators, and our initial experiments have shown promise in this direction, as well.

More generally, datasets are symmetric under groups of general dimensionality, and these groups in general are not commutative. In the case of pixel translations, x and y translations commute with each other, but rotations in the plane (say) do not commute with either of these. We believe the method can also be generalized to noncommutative Lie groups, but this has to be tried and seen.

At 33 dimensions, the datasets are not what one would call "low-dimensional" in the context of symmetry learning (one often encounters, e.g., 2-dimensional datasets that are symmetric under rotations), however, many real datasets have much higher dimensionalities. Our initial experiments indicate that method works on datasets with twice the dimensionality used in this paper, and we think a factor of 3-4 increase in dimensionality should also not be a problem. For dimensions that are orders of magnitude higher, one will likely need further computational, and possibly algorithmic optimizations. In order to try the method on realistic image data, say, one will need to make these optimizations.

Once the model is trained on raw data and the symmetry-equivariant representation (via the group convolution map) is learned, one can utilize the model for other tasks. For instance, one would like to work on a classification task, one can take the representation given by the model and simply train a regular, one-dimensional CNN model on this representation. This is because the representation learned by the model is local and equivariant under "pixel translations" of the usual sort. Whereas it is not obvious what kind of weight sharing is appropriate for a given raw dataset, our model leads to a representation where the usual CNN approach would work.

In this paper, the group actions learned by the model are all linear, i.e., the method learns a *representation* of the underlying group of symmetries by learning a matrix for a discrete generator. However, more generally, symmetry actions can be nonlinear. The philosophy of this paper can be applied to the nonlinear case as well, but of course the practical problems with optimization and the architectural choices for representing a nonlinear map will require work and experimentation.

Finally, let us note that data often has locality directions that are not necessarily symmetry directions. For instance, for the case described in Figure 2, the two orthogonal spatial directions around any point on Earth are locality directions for the temperature distribution, but the system is symmetric only under azimuthal rotations. Our model finds only the representation that has both the locality and the symmetry properties. In particular, there is no direct requirement on the resolving filter for a locality along another direction. Further generalizations along these lines are also possible.

# References

- [1] Taco Cohen and Max Welling. Group equivariant convolutional networks. In *International conference on machine learning*, pages 2990–2999. PMLR, 2016.
- [2] Olivier Babelon, Denis Bernard, and Michel Talon. *Introduction to Classical Integrable Systems*. Cambridge Monographs on Mathematical Physics. Cambridge University Press, 2003.
- [3] Paul J Channell and Clint Scovel. Symplectic integration of hamiltonian systems. *Nonlinearity*, 3(2):231, 1990.
- [4] Krish Desai, Benjamin Nachman, and Jesse Thaler. Symmetry discovery with deep learning. *Physical Review D*, 105(9):096031, 2022.
- [5] Steven Weinberg. What is quantum field theory, and what did we think it is?, 1997.
- [6] Gregory Benton, Marc Finzi, Pavel Izmailov, and Andrew G Wilson. Learning invariances in neural networks from training data. *Advances in neural information processing systems*, 33:17605–17616, 2020.
- [7] David W Romero and Suhas Lohit. Learning partial equivariances from data. *arXiv preprint arXiv:2110.10211*, 2021.
- [8] Sean Craven, Djuna Croon, Daniel Cutting, and Rachel Houtz. Machine learning a manifold. *Physical Review D*, 105(9):096030, 2022.
- [9] Roy T Forestano, Konstantin T Matchev, Katia Matcheva, Alexander Roman, Eyup B Unlu, and Sarunas Verner. Accelerated discovery of machine-learned symmetries: deriving the exceptional lie groups g2, f4 and e6. *Physics Letters B*, 847:138266, 2023.
- [10] Roy T Forestano, Konstantin T Matchev, Katia Matcheva, Alexander Roman, Eyup B Unlu, and Sarunas Verner. Deep learning symmetries and their lie groups, algebras, and subalgebras from first principles. *Machine Learning: Science and Technology*, 4(2):025027, 2023.
- [11] Sven Krippendorf and Marc Syvaeri. Detecting symmetries with neural networks. *Machine Learning: Science and Technology*, 2(1):015010, 2020.
- [12] Gabriela Barenboim, Johannes Hirn, and Veronica Sanz. Symmetry meets ai. SciPost Physics, 11(1):014, 2021.
- [13] Allan Zhou, Tom Knowles, and Chelsea Finn. Meta-learning symmetries by reparameterization. arXiv preprint arXiv:2007.02933, 2020.
- [14] Ian J. Goodfellow, Jean Pouget-Abadie, Mehdi Mirza, Bing Xu, David Warde-Farley, Sherjil Ozair, Aaron Courville, and Yoshua Bengio. Generative adversarial networks, 2014.
- [15] Jianke Yang, Robin Walters, Nima Dehmamy, and Rose Yu. Generative adversarial symmetry discovery. In *International Conference on Machine Learning*, pages 39488–39508. PMLR, 2023.
- [16] Jianke Yang, Nima Dehmamy, Robin Walters, and Rose Yu. Latent space symmetry discovery. *arXiv preprint* arXiv:2310.00105, 2023.
- [17] Rupert Tombs and Christopher G Lester. A method to challenge symmetries in data with self-supervised learning. *Journal of Instrumentation*, 17(08):P08024, 2022.
- [18] Jascha Sohl-Dickstein, Ching Ming Wang, and Bruno A Olshausen. An unsupervised algorithm for learning lie group transformations. *arXiv preprint arXiv:1001.1027*, 2010.
- [19] Nima Dehmamy, Robin Walters, Yanchen Liu, Dashun Wang, and Rose Yu. Automatic symmetry discovery with lie algebra convolutional network. *Advances in Neural Information Processing Systems*, 34:2503–2515, 2021.
- [20] Samuel Greydanus, Misko Dzamba, and Jason Yosinski. Hamiltonian neural networks. *Advances in neural information processing systems*, 32, 2019.
- [21] Ferran Alet, Dylan Doblar, Allan Zhou, Josh Tenenbaum, Kenji Kawaguchi, and Chelsea Finn. Noether networks: meta-learning useful conserved quantities. *Advances in Neural Information Processing Systems*, 34:16384–16397, 2021.
- [22] JL Doob. Stochastic Processes. Wiley, 1991.
- [23] Anthony J Bell and Terrence J Sejnowski. An information-maximization approach to blind separation and blind deconvolution. *Neural computation*, 7(6):1129–1159, 1995.
- [24] Georg Pichler, Pierre Jean A Colombo, Malik Boudiaf, Günther Koliander, and Pablo Piantanida. A differential entropy estimator for training neural networks. In *International Conference on Machine Learning*, pages 17691– 17715. PMLR, 2022.
- [25] T.M. Cover. *Elements of Information Theory*. Wiley series in telecommunications and signal processing. Wiley-India, 1999.

# **A Probability Estimation**

## A.1 Marginal probability estimator

We use probability estimators proposed in the work of [24]. We use weighted sum of gaussian kernels parametrized by their means  $\mu$  and standart deviations  $\sigma$ 

$$\hat{f}_{i}(y_{i}) = \frac{1}{M} \sum_{m=1}^{M} w_{im} \mathcal{K}(\mu_{im}, \sigma_{im})$$
(27)

while M is the number of kernels for each estimator and w is the weight of each kernel for modeling probability density<sup>21</sup>. Gaussian kernel is defined as

$$\mathcal{K}(\mu, \sigma) = \frac{1}{\sigma\sqrt{(2\pi)}} \exp\left(-\frac{1}{2\sigma^2}(x-\mu)^2\right)$$
 (28)

while the probability density estimator is trained by minimizing the estimated entropy  $\hat{h} = -\mathbb{E}[\log(\hat{f}_i(y_i))]$ .

## A.2 Conditional probability estimator

**Overview** We use the differential conditional probability estimator proposed in the work of [24] with few extensions that are added to improve stability and computational efficiency. The proposed method involves the use of a neural network to estimate the parameters of the Gaussian mixture Theta given the input of the network. When applied without modification, method requires three neural networks for each input i and output j giving the following probability estimation

$$\hat{f}(y_j|y_i) = \frac{1}{M} \sum_{m=1}^{M} w_{jim}(y_i) \mathcal{K}(\mu_{jim}(y_i), \sigma_{jim}(y_i))$$
 (29)

while  $w_{ji}$ ,  $\mu_{ji}$  and  $\sigma_{ji}$  corresponds set of neural networks and  $\mathcal{K}$  is the gaussian kernel parametrized with  $\mu$  and  $\sigma$  values. Training is accomplished by minimizing  $\hat{h} = -\mathbb{E}[\log(\hat{f}(y_j|y_i))]$  for each i and j while  $i \neq j$ .

The major difficulty arising in our application is the high number of input and output parameters. Applying this estimator in a straightforward manner would require  $3 \times d^2$  small neural networks, which are quite inefficient. By using single-input multiple-output neural networks, this can be decreased to  $3 \times d$  neural networks. Although this is a significant improvement, it still introduces a performance bottleneck.

In order to improve the performance of the estimator, we have used 3 neural networks with a specific masking procedure. The masking procedure consists of masking the inputs(given parameters) such that only one of the components is kept as is for each sample and the rest is set to zero. More precisely, for each sample n, we mask all components except the component i while  $n \equiv i \pmod{d}$ . The probabilities for other components are estimated using the given input. As a result, 3 networks are shared to estimate all conditional probabilities without introducing quadratic complexity.

Denoting the j'th outputs of the neural networks with  $w_j$ ,  $\sigma_j$  and  $\mu_j$  while j and k we can express the resultant conditional probability estimation as given below

$$\hat{f}_{j|i}(y_j|y_i) = \frac{1}{M} \sum_{m=1}^{M} w_{jm}(\mathbb{1}_{i}\mathbf{y}) \mathcal{K}(\mu_{jm}(\mathbb{1}_{im}\mathbf{y}), \sigma_j(\mathbb{1}_{i}\mathbf{y}))$$
(30)

while the sample vector  $\mathbf{y}$  with the indicator function  $\mathbb{1}_i$  represents the masking procedure. Tailored according to the masking procedure, we train the model by minimizing  $\hat{h} = -\mathbb{E}[\log(\hat{f}_{j|i}(y_j|y_i))]$  for each i and j while  $i \neq j$  similarly.

<sup>&</sup>lt;sup>21</sup>Weights constrained such that they satisfy  $\sum_{m} w_{im} = 1$ .

<sup>&</sup>lt;sup>22</sup>Indicator function gives a vector whom components are zero except the *i*'th component  $(\mathbb{1}_i = (0, 0, \dots, 1, \dots, 0))$ . It should be mentioned that there is a hidden dependency between selection of *i* and *n* since the estimation is made only for  $n \equiv i \pmod{d}$  for each sample *n* as mentioned previously.

**Architecture** The conditional probability estimator consists of three neural networks to parameterize gaussian mixture parameters. Each of the networks is identical except for the output activation functions they have used.

Each of the neural networks is composed of d input,  $4 \times d \times M$  hidden, and  $\times d \times M$  output neurons, while there are two hidden layers. While the input corresponds to the value of each component, output corresponds to the flattened version of the tensor involving parameters for four different gaussian kernels specifying each components conditional probability distribution. We have used the LeakyReLU activation function with  $\alpha=0.1$  at the output of each layer except the last one. The output activation functions for the three neural networks are given in the table 3.

Estimated quantity	Output activation function
Kernel weights	Softmax over the kernels axis
Mean value of each kernel	No (linear) activation
Variances of each kernel	Scaled tangent hyperbolic
	function followed by exponentiation

Table 3: Activation functions for conditional probability estimator

# B Equivariance of Group convolution

Plugging  $\rho_{\mathcal{X}}(u)\mathbf{f} \to \mathbf{f}$  while  $u \in G$ 

$$[(\rho_{\mathcal{X}}(u)\mathbf{f}) \star \mathbf{h}](g) = \langle \rho_{\mathcal{X}}(u)\mathbf{f}, \rho_{\mathcal{X}}(g)\mathbf{h} \rangle_{\mathcal{X}}$$
(31)

$$= \langle \mathbf{f}, \rho_{\mathcal{X}}(u^{-1})\rho_{\mathcal{X}}(g)\mathbf{h} \rangle_{\mathcal{X}}$$
(32)

$$= \langle \mathbf{f}, \rho_{\mathcal{X}}(u^{-1}g)\mathbf{h} \rangle_{\mathcal{X}} \tag{33}$$

$$\implies [(\rho_{\mathcal{X}}(u)\mathbf{f}) \star \mathbf{h}](g) = [\mathbf{f} \star \mathbf{h}](u^{-1}g)$$
(34)

$$= \rho_G(u)[\mathbf{f} \star \mathbf{h}](g) \tag{35}$$

while  $\rho_G:G\to G$  is the representation of the group that acts on the group itself. In the last line, we have defined the group action over the functions of the group elements as  $\rho_G(u)k(v)=k(u^{-1}v)$  while  $k:G\to\mathbb{R}$  for convenience. Consequently, any action of the group on the input leads to the corresponding translation at the output.

## C Mutual Information Maximization between Input and Output

We can express mutual information between the input random vector  $\mathbf{X}$  and output random vector  $\mathbf{Y}$  as

$$I(X,Y) = h(Y) - h(Y|X).$$
 (36)

Since we use a deterministic map,  $h(Y|X) = -\infty$  unless we add noise to the output. Considering that adding tiny amount of gaussian noise to the output map wouldn't change anything practically, we modify the equation as;

$$I(X,Y) = h(Y) - h_0 (37)$$

while  $h_0$  corresponds to the entropy of the gaussian noise added to the output. Since  $h_0$  is a constant, it would not affect the gradients or higher-order derivatives. Consequently, maximizing output entropy h(Y) is equivalent to maximizing mutual information I(X,Y) between input  $\mathbf{X}$  and output  $\mathbf{Y}$ .

## D For Markov fields, Output Representation is a Markov Field

In order to analyze the composed effect of these two terms, we can expand the joint entropy using the chain rule for entropies.

$$h(\mathbf{Y}) = \sum_{i=1}^{d} h(Y_i | Y_{< i})$$
(38)

while  $Y_{< i}$  is set of component random variables  $\{Y_1, Y_2, \dots Y_{i-1}\}$  when i > 1. For i = 1, it means that no conditioning is applied. We define the following form of entropy approximation which only considers local dependencies

$$h^{(m)}(\mathbf{Y}) = \sum_{i} h(Y_i | X_{[i-1,i-m]})$$
(39)

while  $Y_{[i-1,i-m]}$  is the set of random variables  $\{Y_{i-m},Y_{i-m+1},\ldots Y_{i-1}\}$  when  $m\geq 1$ . m=0 corresponds to the case in which no conditioning is applied.

Since conditioning can only reduce entropy<sup>23</sup> we have the following relation.

$$h(\mathbf{Y}) \le h^{(d-1)}(\mathbf{Y}) \le \dots \le h^{(1)}(\mathbf{Y}) \le h^{(0)}(\mathbf{Y})$$
 (40)

By minimizing Total correlation  $C = h^{(0)}(\mathbf{Y}) - h(\mathbf{Y})$ , we enforce all conditional entropies to be equal which is only possible when they are independent. However, when we add alignment regularization as well, we also maximize mutual information between adjacent timesteps which is given by  $I(Y_i, Y_{i+1})$ 

$$I(Y_i, Y_{i+1}) = H(Y_{i+1}) - H(Y_{i+1}|Y_i)$$
(41)

which correponds to maximizing entropies  $H(Y_{i+1})$  while minimizing conditional entropies  $H(Y_{i+1}|Y_i)$ . If the Total correlation regularization is dominant, net effect becomes minimizing both  $h^{(0)}(\mathbf{Y})$  and  $h^{(1)}(\mathbf{Y})$  while maximizing  $h(\mathbf{Y})$ . Assuming that these loss terms are maximally satisfied, we have  $h(\mathbf{Y}) = h^{(d-1)}(\mathbf{Y}) = \cdots = h^{(1)}(\mathbf{Y}) < h^{(0)}(\mathbf{Y})$  while  $h^{(1)}(\mathbf{Y}) < h^{(0)}(\mathbf{Y})$  since we minimized conditional entropies due to maximizing correlation between adjacent components forcing entropy to be smaller than the independent case. This corresponds to the case where the learned representation resembles the Markov field of first order. Besides, due to the uniformity regularization term, we also have a stationary Markov field as well.

# E For Markov fields, Underlying Signal is Revealed.

To prove this, we first express the input as a random vector  $\mathbf{X}$ 

$$X_j = \sum_p M_p \left[ \sum_i x_i^0 G_{ij}^p \right] \tag{42}$$

while  $(M_1, M_2, \dots M_d)$  is the random field over the hidden Lie manifold which taken to be discrete for convenience. And the random vector corresponding to output representation **Y** is expressed as

$$Y_{q} = \sum_{j} X_{j} L_{jq} = \sum_{j,k} X_{j} (G^{T})_{jk}^{q} \psi_{k}^{0}$$
(43)

$$= \sum_{p} M_{p} \left[ \sum_{i,k} x_{i}^{0} G_{ik}^{p-q} \psi_{k}^{0} \right]$$
 (44)

Now we may consider the  $\sum_{i,k} x_i^0 G_{ik}^{p-q} \psi^0_k$  term as a linear map which maps the signals in hidden Lie manifold to observable output representation. Defining  $K_{pq} \triangleq \sum_{i,k} x_i^0 G_{ik}^{p-q} \psi^0_k$  we can write the output as

$$Y_q = \sum_p M_p K_{pq} \tag{45}$$

In reality K has Toeplitz structure, but if it is a big matrix, we can approximate it with a circulant one. Let r be the number of elements in each column that is different from zero. Then each component of the output representation would depend on the r points in the hidden manifold. For the output representation to satisfy the first-order Markov field property, each  $Y_{i-1}$  and  $Y_{i+1}$  should be conditionally independent given  $Y_i$ . This is only possible if  $Y_i$  fixes the common dependency terms of  $Y_{i-1}$  and  $Y_{i+1}$  or  $Y_{i-1}$  and  $Y_{i+1}$  don't have common dependency terms at all.

For r>1, we see that  $Y_i$  cannot fix any dependency terms since there is more than one dependency term to fix but only one equation. So for a lifted representation to have a first-order Markov property, the only remaining option is  $Y_{i-1}$  and  $Y_{i+1}$  not having common dependencies. However, due to the circulant nature of K, it is inevitable that some rows have common dependencies if r>1. Consequently, we see that the output representation does not resemble a first-order Markov field unless K has a very sparse structure. Precisely, the mentioned considerations limit K to be a left or right circulant matrix with only one non-zero element. Such a matrix is limited to reflections and changing the polarity of an input, which is also validated in all our experiments.

<sup>&</sup>lt;sup>23</sup>For more information about fundamentals of information theory, refer to [25].

# **Effects of Orthonormal Transformation**

Based on the data model 3.1, we can prove that the application of orthonormal transformation leads to a similar symmetry learning problem while the representation to be revealed  $\hat{f}_{np}$  remains the same. Multiplying ?? with  $Q \in \mathbb{R}^{d \times d}$  from the left, we obtain the following

$$\mathbf{x}_{n}Q = \mathbf{x}^{(0)} \sum_{p} \hat{f}_{np} \rho_{\mathcal{X}}(\mathfrak{G}^{p}) Q + \tilde{\mathbf{x}}_{n} Q$$

$$\mathbf{x}_{n}Q = \mathbf{x}^{(0)} \sum_{p} \hat{f}_{np} Q Q^{T} \rho_{\mathcal{X}}(\mathfrak{G}^{p}) Q + \tilde{\mathbf{x}}_{n} Q$$

$$\tag{47}$$

$$\mathbf{x}_n Q = \mathbf{x}^{(0)} \sum_{p} \hat{f}_{np} Q Q^T \rho_{\mathcal{X}}(\mathfrak{G}^p) Q + \tilde{\mathbf{x}}_n Q$$
(47)

$$\mathbf{x'}_{n} = \mathbf{x'}^{(0)} \sum_{p} \hat{f}_{np} \tilde{\rho}_{\mathcal{X}}(\mathfrak{G}^{p}) + \tilde{\mathbf{x}}'_{n}$$
(48)

while primed vectors correspond to the original vectors multiplied with the orthonormal matrix Q. In this new symmetry learning problem, the representation of the generator is related to the natural case via a similarity transformation  $\tilde{\rho}_{\mathcal{X}}(\mathfrak{G}^p) = Q^T \rho_{\mathcal{X}}(\mathfrak{G}^p) Q.$